CHAPTER 1

Introduction to Quantum Information Science

1.1. Background

Quantum Information Science is the amalgamation of Computer Science, Quantum Physics, and Information Theory, so we will begin by looking at the relevant history of these three fields.

At the turn of the 20th Century physicists were trying to explain a plethora of phenomena and experimental results using classical Newtonian based physics, but were not producing fruitful or satisfactory solutions. Specifically, the characteristic absorption and emission of electromagnetic waves by atomic gasses, the structure of an atom, the characteristic black body spectrum at low temperatures, and the photoelectric effect were the most prominent. In all respects classical physics could not explain these phenomenon, and Max Plank, in a stroke of pure genius, or perhaps desperate luck, started a physics revolution. He questioned the fundamental assumption that energy is always a continuous quantity, and instead postulated that the energy of a harmonic oscillator is a multiple of a smallest quantum unit of energy. With this idea he was able to properly explain the black-body radiation spectrum. Then Einstein used the quanta idea to explain the photoelectric effect, and Bohr used it with de Broglie's matter wave hypothesis to explain the stability of atoms. A small snowball was set in motion down the mountain of physics leading to the successful explanation of all of these phenomena and more, as well as the formal construction of Quantum Mechanics. Quantum Mechanics is governed by a few postulates which may be stated differently in different context, but four core postulates for our concerns will be

(1) The complete state of a physical system is described by a complex wave function (equivalently a vector in Hilbert Space) $\Psi(r,t)$, which is square integrable and normalizable i.e. $1 = \int_{\text{all space}} |\Psi|^2$.
(2) The time evolution of any closed system is described by the time-dependent Schrodinger equation $\hat{H}\Psi = i\hbar\frac{d}{dt}\Psi$ and is assumed to evolve unitarily.
(3) The measurement postulate states that all dynamical variables can be represented by a linear Hermitian operator with eigenvalues λ_i and eigenvectors $|\lambda_i\rangle$. The outcome of a measurement will always be one of the eigenvalues with probability $|\langle\lambda_i|\Psi\rangle|^2$and the measurement will reduce the state of the system from $|\Psi\rangle$ to $|\lambda_i\rangle$.
(4) Composite quantum system are completely described by the tensor product[1] of the system component states. $|\Psi_{12}\rangle = |\Psi_1\rangle \otimes |\Psi_2\rangle$

These postulates have been innumerably successful at explaining the world, but the consequences are not always easy to understand, or calculate. In fact, one of the reasons to build a quantum computer, which is governed by these postulates, is to attempt to better simulate and calculate large and complex quantum systems that can not be easily solved by hand or efficiently with a classical computer.

One may argue about when Computer Science actually began as it is a science for performing computations and computational algorithms and instruments have been around for centuries. However, for our purposes we will go back only as far as 1936 when Turing gave a general definition of a programmable computing machine called a Universal Turing Machine that in many regards is a theoretical model for the modern computer. Based on an infinite string of memory tape and a few principle set of operations, Turing demonstrated that such a machine could solve any problem that could be solved "algorithmically". Independently around the same time Alonzo Church, created a lambda calculus for defining functions, as we would know them in computer programing, and showed that these functions could be solved "algorithmically".

[1] $\begin{bmatrix} a_{12} \\ a_{22} \end{bmatrix} \otimes \begin{bmatrix} b_{12} \\ b_{22} \end{bmatrix} = \begin{bmatrix} a_{12}\begin{bmatrix} b_{12} \\ b_{22} \end{bmatrix} \\ a_{22}\begin{bmatrix} b_{12} \\ b_{22} \end{bmatrix} \end{bmatrix} = \begin{bmatrix} a_{12}b_{12} \\ a_{12}b_{22} \\ a_{22}b_{12} \\ a_{22}b_{22} \end{bmatrix}$

Together they formed the Church-Turing thesis, one of the basis concepts in modern computing science, in which the strong version is now stated as: *any algorithmic process that can be executed on any hardware can be simulated efficiently on a Turing machine.* Efficiently meaning in polynomial time dependent on input size, as opposed to super-polynomial time, usually exponential. In fact there are many versions of this thesis, many interpretations and extensions, as well as a built-in ambiguity to the definitions used in the thesis. Regardless, the Church-Turing thesis is a legitimate starting point for the desire to create a Universal Turing machine, which in many regards is the modern computer. Around this time, John Von Neumann defined the basic components necessary for realizing such a computer for practical use. It was another 10 years however, until the transistor was first developed at Bell Labs and development for modern, fast, small and low cost computers would be realized. Soon after that the development of computers followed Moore's law which follows an exponential increase in the number of transistors on a processing unit of equal size. For many decades we have achieved this, but finally the limits of current CMOS technology have been reached and a hunt for newer materials and architectures has begun.

Finally, Information and Communication theory began with a paper in 1948 by Claude Shannon in which a mathematical framework was formalized for the concept of "information". With this framework he worked out two fundamental theorems in information theory. The first demonstrates the required resources necessary for communication and storage of information in the absence of noise in the communication channel. The second theorem defines a limit of reliable information which can be sent over a channel in the presence of noise. This lead to the development of error-correction codes central to modern communication. When scientists began wondering what these theorems might look like if subject to quantum laws, they found some startling and exciting results. These include things like the *no-cloning theorem, teleportation,* and bizarre behavior like non-zero capacity for communication between two nodes through two quantum channels in opposite directions, each individually with zero communication capacity due to noise.

Another offshoot of this field, though established well before it, is cryptography or the transmission of information securely and secretly. In the pursuit of creating more and more secure forms of cryptography, cytologists were naturally led to quantum based system, were information seems inherently secure. A common concern for secure transmission of information is the Man-In-The-Middle attack in which an eavesdropper sits on the channel of communication and listens to the information being sent. You might be able to encrypt the communication so that the eavesdropper can not understand what is being said, but in most forms of encryption a key has to be shared between the two parties, and physically sharing the key is not always an option. In this case if the man in the middle is there from the beginning and catches the key, he can decrypt everything. Well, due to the nature of quantum mechanics, this attack appears nullified since once a "measurement" of the information is taken it is irreversibly lost and can not be copied. If an eavesdropper is in the channel, the information will never be received by the intended receiver, since it will be destroyed by the eavesdropper. A proper communication protocol will notice this and stop transmission. Today, simple quantum devices have been built to distribute keys between two sources securely. Do not think that this is the conclusion to the field of cryptography, on the contrary it is really just the beginning of a new era, a quantum era. Significant advances and understanding are necessary to better harness quantum cryptographic power as well as understand its limitations.

It was only after the maturity of these three fields and advances in technology and understanding of quantum systems that Quantum Information Science could really come to fruition. Particularly, advances in controlling and measuring the state of single particles, hitting the limits of current computing technology, the discovery of superconducting materials, refrigeration technology, laser technology, ion trapping, etc have all made QIS and quantum computation actually possible. So the question now is what is QIS?

1.2. Quantum Information Science

Quantum information science is a broad field encompassing all things related to computation, communication, storage, encryption, etc. which are based on the laws of quantum mechanics. It also tries to formulate procedures and suggest experiments to better understand basic properties of quantum systems and develop intuition for the predictions of quantum mechanics through experiments.

One of the first events to shape the field of QIS can be traced back to a paper in 1982 by Richard Feymann in which he stated that a computational device based on the laws of quantum mechanics could most effectively simulate large scale quantum systems. Though a classical computer can simulate quantum systems, it does so incredibly inefficiently. The biggest inefficiency is that a classical computer inherently

stores classical information and classically there is nothing like a superposition state. However, a computer based on quantum mechanics storing quantum information in a quantum bit, inherently has the ability to be in superposition states as well as entangle with other qubits naturally.

The next major step came in 1985 when David Deutsch was searching for a device that could efficiently simulate an arbitrary physical system. His main goal was to disprove the strong Church-Turing thesis and find something more powerful then a Universal Probabilistic Turing Machine. According to physics, nature is inherently quantum mechanical and follows the quantum postulates, so naturally Deutsch proposed a quantum mechanical based system, a quantum computer. If this was all he did it would not be all that impressive, but in fact he was able to show that in a particular case the use of quantum mechanics allowed a computation speed up over a classical computation. This was the first quantum algorithm, and it is provably a factor of 2 times faster than any classical computation.

The algorithm itself determines if a function is "balanced" that is the left side of an equation is equal to the right side. Now classically this can be done by calculating the left side, and right side independently then comparing the results. However, with the power of quantum superposition, the quantum computer can basically calculate both sides simultaneously, thereby requiring only one calculation instead of two. Unfortunately, this is not a major increase in speed, nor is it a terribly interesting problem from a computer scientist stand point. However, it is a proof of concept that quantum computers can be more powerful than classical ones.

Over the next decade Deutsch and others improved and discovered a few more quantum algorithms that were provably faster than the classical counterparts. However, the largest breakthrough came in 1994 when Shor developed a quantum algorithm that efficiently finds prime factors. The difficulty in factoring large number is the basis of many encryption models. One such encryption model is RSA and is used widely around the world to securely encrypt information, including government communications. The best known classical algorithm to factor a 5,000 digit number with 1ns per instruction speed would takes on the order of 5 trillion, yes trillion, years to solve. Using a quantum computer, of equal speed and with the use of Shor's algorithm, may require just over 2 minutes. That is a significant speed increase on a significant computer science problem. It has yet to be proven that there is some undiscovered classical algorithm out there that can beat Shor's algorithm, so in that respect the race is still on. However, since then I think there has be significantly larger interest and money to create a quantum computer.

There have been a few other key algorithms created that are provably faster than classical ones, including Grover's search algorithm, but unfortunately these algorithms are often for problems with unknown or unimportant applications. The search for efficient and useful quantum algorithms is a large and difficult problem in the field of QIS. Quantum algorithms are often adverse to intuition and common everyday experiences. No one yet even knows why, or what particular aspect of quantum computing might make it stronger than classical computing. Also, quantum computing is in its infancy while classical computing has had many decades of research and huge quantities of money in advancing the technology. For a quantum algorithm to be interesting it has to beat, and probably significantly beat classical algorithms, which is no easy task. Of course we are also limited by the physical realization of a quantum computers to test these algorithms and perhaps create new ones. To date Shor's algorithm has been experimentally realized up to factoring 21, far from practical use.

1.3. General Quantum Computation and Qubits

A lot more could be said about the history of Quantum Information Science, but the major point of this course is to learn about the many physical systems which have realized basic quantum computation. First, we will cover the general characteristics of quantum computation which must ultimately be realized by any physical system that is to successfully become a quantum computer of sorts. In 2000, David DiVincenzo, while working at IBM, published a paper outlining the necessary criteria for a physical system to successfully implement quantum information processing. The 5 core criteria are

(1) A ***scalable*** physical system with well characterized qubits
(2) The ability to ***initialize*** the state of the qubits
(3) ***Long coherence*** times, much longer than the gate operations time
(4) A ***universal*** set of ***quantum gates*** with high fidelity
(5) Qubit-specific ***measurement*** capabilities

He also added two supplementary criteria relating to the transmission and movement of information:

(6) The ability to ***convert*** from stationary to mobile, "flying" qubits and back.
(7) The ability to ***faithfully transmit*** flying qubits from one location to another.

These criteria laid out by DiVincenzo will be our guiding light for analyzing physical systems to determine if they are capable of becoming scalable universal quantum information processing systems. However, before we get into the physical systems, these criteria bring up some general terms which we can discuss first. Namely, the concept of a "qubit", "gates", "measurement", and "coherence".

A qubit is what you would expect, a quantum bit of information. As a comparison, a classical bit is quite easy to understand, as the smallest unit of information a bit has two possible values, 0 or 1. Of course this could also be represented as "on" or "off", "true" or "false", "up" or "down", "heads" or "tails". That is to say it is defined by two non-coexistent logical states and the classical bit can only ever be in one state or the other. In a modern physical realization of a classical bit, the "bit" is normally a level of voltage across a particular element representing the bit in an electrical circuit. This could be across a capacitor or a transistor, etc. A quantum bit is realized in a quantum mechanical system with two distinct states, much like a classical bit, but due to the superposition ability of quantum mechanical systems a qubit can exist in a continuum of possibilities between and including 0 and 1.

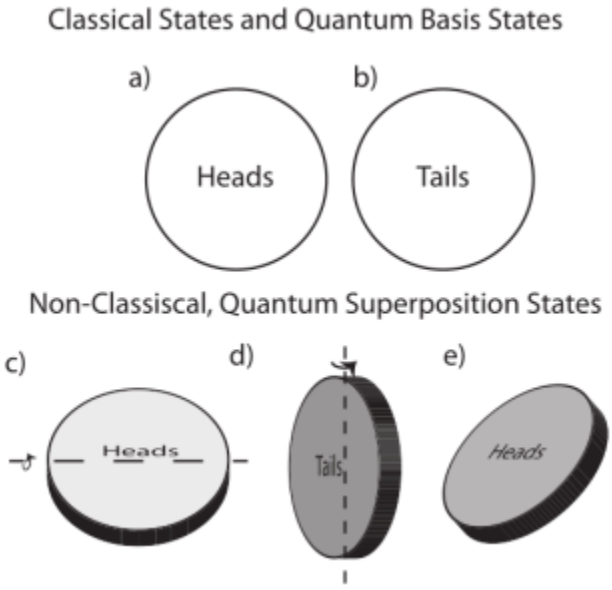

FIGURE 1.3.1. Visuals of coin states representing classical and quantum states. a) and b) are classical states and also quantum pure basis states. c) and d) are quantum superpositions states which can occur via rotations about these two orthogonal axes. e) another quantum superposition state composed of two rotations, one about each rotation axis.

This superposition of states is one of the key differences between a classical bit and a quantum bit. As an analogy to try to conceptualize this difference we will think of a coin in two different contexts. The first context is a classical one in which a very thin, but radially large, coin falls near the surface of the earth. When we release the coin it will always fall towards the ground and end up in a state of heads or tails, or if we precisely control the fall, we can cause the coin to end up in a heads or tails state. The end result, however, is always the coin on the ground with either heads or tails facing up. The second context is the same coin in a special laboratory, which, to the best of its ability, has found a way to nullify earth's gravitation field inside a box. In this box we can control the orientation of the coin by rotating it about any axis perhaps with precisely controlled air jets on the inside of the box. In this context the the coin is in a continuum of states between heads and tails and also in 2 different dimensions. That is to say that rotations between heads and tails can occur around 2 perpendicular axis that line in the thickness of the coin, while rotations around an axis through the face of the coin does not change the amount of "heads" or "tails" the state of the coin is in.

One could imagine a unit vector normal to the face of the "heads" side of the coin and recognize that the vector can sweep out a unit sphere. In fact, we will use this concept of a vector in a unit sphere to visualize the general state of a single qubit. The sphere in this context is called a Bloch sphere. The general state of the qubit can be written mathematically as

$$|\Psi\rangle = \alpha\,|0\rangle + \beta\,|1\rangle \tag{1.3.1}$$

where α and β are complex numbers which allow for the two dimensionality of rotations and $|0\rangle$, $|1\rangle$ are generalized "computational" basis states of the system. We could have easily used $|\text{Heads}\rangle$and $|\text{Tails}\rangle$, spin up and down, existence and non-existence etc. Any quantum mechanical system with two orthogonal states can define the basis states of the system. Typically, this is two distinct levels of energy quantized by some

quantum mechanical dynamics, such as a harmonic potential, or spin states in a magnetic field. The first postulate of quantum mechanics tells us that $|\Psi\rangle$ must be normalizable so we have the constraint that $|\alpha|^2 + |\beta|^2 = 1$. Using the Bloch sphere context we can write $|\Psi\rangle$ in the most general case in terms of spherical coordinates as

$$|\Psi\rangle = e^{i\gamma}\left(\cos\frac{\theta}{2}|0\rangle + e^{i\phi}\sin\frac{\theta}{2}|1\rangle\right) \tag{1.3.2}$$

where γ, θ, and ϕ are all real numbers. The angles θ and ϕ are defined in Figure 1.3.2. Typically, the global phase $e^{i\gamma}$ is omitted because it has no observable effects on single qubit observables. This gives the relations

$$\alpha = \cos\frac{\theta}{2} \qquad \beta = e^{i\phi}\sin\frac{\theta}{2} \tag{1.3.3}$$

The angles θ correspond to rotations of the state vector in the x-z plane while the ϕ rotations correspond to rotations of the state vector in the x-y plane. The equator of the Bloch sphere correlates to an equal superposition of the two basis states $|0\rangle$ and $|1\rangle$ such that $|\alpha|^2 = |\beta|^2 = \frac{1}{2}$ and the wave function has the general form $\frac{1}{\sqrt{2}}\left(|0\rangle + e^{i\phi}|1\rangle\right)$. You may be wondering why we have defined the system with an angle of $\theta/2$ instead of just θ, this is due to the fact that a quantum mechanical two-level system is actually periodic with 4π rotations. Mathematically, $|\Psi\rangle_{\theta=0} = -|\Psi\rangle_{\theta=2\pi} = |\Psi\rangle_{\theta=4\pi}$.

The basis states are the eigenvectors of the chosen reference frame and are ultimately the observable states of that basis. If we "measure" the state of the coin in the computational basis we will only ever find it in the "tails" or "heads" state, a 0 or 1 state with probability $|\alpha|^2$and $|\beta|^2$ respectively. This is a consequence of the measurement postulate and the "collapse" of the quantum wave function into a classical observable variable. We will address the "measurement" issue a little later. Of course we could measure the system in some other basis, but the results will only ever be the eigenvectors of that basis.

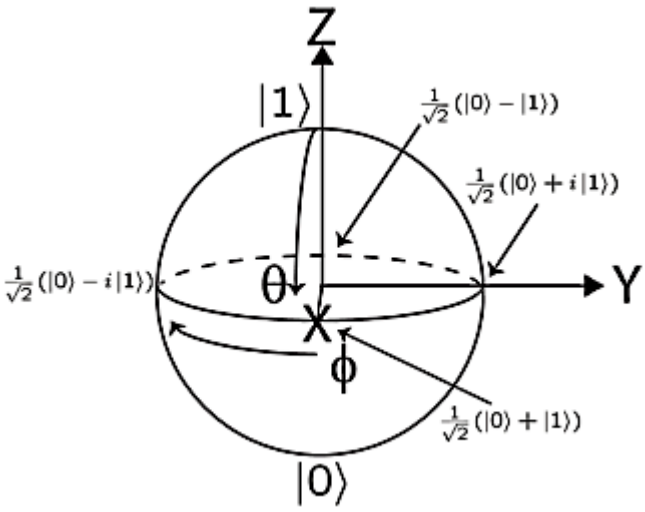

FIGURE 1.3.2. The Bloch Sphere is a physical representation of the state of a single qubit

Returning to the coin in a special box analogy, it is as if the only way to determine the state of the coin is to open the box and break the seal protecting the coin from earth's gravity. This causes the coin to fall to the ground and obtain either a "heads" or "tails" state. The quantum state before the box is opened will probabilistically determine the "measured" state of the coin. That is the α's and β's tell you how likely the coin is to be oriented when it hits the ground. The power of the quantum computer is not in the measurement results, it is in the new possibilities of dynamics that can occur when the coins are in that delicate floating state. Ultimately, when we are considering a computation the end result of algorithms should be the same, but *how* the algorithm is done is what separates degrees of functionality. The fact that a quantum computer can ultimately do anything a classical computer can do and more, suggests the power of quantum computing, especially when we consider the fact that the theory of quantum mechanics has been more successful at explaining the natural world than has classical physics.

In summary a classical bit is only ever in two states, which we can think of as a vector which points either up or down. A quantum bit on the other hand is a vector that can be in any state on the Bloch sphere. A classical bit follows the laws of classical mechanics, while a quantum bit follows the laws of quantum mechanics. A classical bit can only exist in either of two non-coexistent logical states, while a quantum bit can exist in an arbitrary superposition of both of these states.

1.4. Qubit Manipulations and Gates

The second DiVincenzo criteria tells us that we need to be able to initialize our qubits. Using our qubit model of the Bloch sphere, this means most simply that we need to be able to put our qubit vector into any position on that sphere. It should be quite easy to convince yourself that there are 4 unique rotation operations which allow the vector to transform from any state into any other state in the Bloch sphere. These 4 rotations operations are rotations about each Cartesian axis, and an identity rotation which does not alter the vector. In fact, with a little thought you will see that only two rotation axis are required for universal state creation.

The language of quantum mechanics is Linear Algebra and the dynamics are governed by the time dependent Schrodinger equation

$$i\hbar\frac{d}{dt}|\Psi\rangle = \hat{H}|\Psi\rangle \tag{1.4.1}$$

the general solution for a *time-independent* Hamiltonian is

$$|\Psi(t)\rangle = \exp\left(-\frac{i}{\hbar}\hat{H}t\right)|\Psi_0\rangle \tag{1.4.2}$$

where $|\Psi_0\rangle$ is the initial state of the system. Our rotation transformations will occur as a result of our Hamiltonian operator being exponentiated. As it turns out, the Pauli matrices when exponentiated are perfect rotation matrices about the respective axis. Specifically, the Pauli matrices are

$$\hat{\sigma}_I = \begin{bmatrix} 1 & 0 \\ 0 & 1 \end{bmatrix} \qquad \hat{\sigma}_X = \begin{bmatrix} 0 & 1 \\ 1 & 0 \end{bmatrix} \qquad \hat{\sigma}_Y = \begin{bmatrix} 0 & -i \\ i & 0 \end{bmatrix} \qquad \hat{\sigma}_Z = \begin{bmatrix} 1 & 0 \\ 0 & -1 \end{bmatrix} \tag{1.4.3}$$

but when exponentiated we find

$$R_I(\Theta) = e^{-i\Theta\hat{\sigma}_I/2} = \begin{bmatrix} e^{-i\Theta/2} & 0 \\ 0 & e^{-i\Theta/2} \end{bmatrix} \qquad R_X(\Theta) = e^{-i\Theta\hat{\sigma}_X/2} = \begin{bmatrix} \cos\frac{\Theta}{2} & -i\sin\frac{\Theta}{2} \\ -i\sin\frac{\Theta}{2} & \cos\frac{\Theta}{2} \end{bmatrix} \tag{1.4.4}$$

$$R_Y(\Theta) = e^{-i\Theta\hat{\sigma}_Y/2} = \begin{bmatrix} \cos\frac{\Theta}{2} & -\sin\frac{\Theta}{2} \\ \sin\frac{\Theta}{2} & \cos\frac{\Theta}{2} \end{bmatrix} \qquad R_Z(\Theta) = e^{-i\Theta\hat{\sigma}_Z/2} = \begin{bmatrix} e^{-i\Theta/2} & 0 \\ 0 & e^{i\Theta/2} \end{bmatrix}$$

You can check the math for yourself as you please. As a quick example a $\Theta = \pi$ rotation about the y axis, should intuitively flip the qubit from 0 to 1. Using for our basis states $|0\rangle = \begin{bmatrix} 0 \\ 1 \end{bmatrix}$ and $|1\rangle = \begin{bmatrix} 1 \\ 0 \end{bmatrix}$ such that

$$R_Y(\pi)|0\rangle = \begin{bmatrix} 0 & -1 \\ 1 & 0 \end{bmatrix}\begin{bmatrix} 0 \\ 1 \end{bmatrix} = \begin{bmatrix} -1 \\ 0 \end{bmatrix} = -|1\rangle$$

This is simply a global phase factor which can be ignored in the single qubit case. These rotation matrices will inevitably change the values of α and β and rotate our qubit vector around the Bloch Sphere. The take away message here, however, is that *a Hamiltonian with Pauli operators present indicates a physical system allowing for complete single qubit initialization and manipulation.* We therefore have some kind of guide for what to look for in a physical system for single qubit manipulation.

There are 4 special rotation transformations which we should note as they are common to see in circuit diagrams and quantum science texts. These are the Pauli X, Y and Z gates as well as the Hadamard gate. The Pauli gates are simply transformation matrices equivalent to the original Pauli matrices. The Pauli X gate is like a classical NOT operation and maps the states $|0\rangle \to |1\rangle$ and $|1\rangle \to |0\rangle$. It corresponds to a π rotation about the X axis on the Bloch sphere. The Pauli Y gate is known as a conjugate bit flip in that it maps the states $|0\rangle \to i|1\rangle$ and $|1\rangle \to -i|0\rangle$ and is a π rotation about the Y axis on the Bloch sphere. The Pauli Z gate is a phase flip gate in that it leaves the $|0\rangle$ state unchanged but $|1\rangle \to -|1\rangle$. This is also a π rotation about the Z axis on the Bloch sphere. Finally, we have the Hadamard gate which puts the qubit onto the equator of the Bloch sphere in a superposition state. Specifically, $|0\rangle \to 1/\sqrt{2}(|0\rangle + |1\rangle)$ and $|1\rangle \to 1/\sqrt{2}(|0\rangle - |1\rangle)$. This is equivalent to a π rotation about the $(1, 0, 1)$ axis or the $1/\sqrt{2}(\vec{x} + \vec{z})$ axis. The Hadamard transformation matrix is $\frac{1}{\sqrt{2}}\begin{bmatrix} 1 & 1 \\ 1 & -1 \end{bmatrix}$. These are all single qubit gates.

The next thing we need to find are quantum gates which act on two or more qubits. Mathematically, a quantum gate is simply an operator that acts on the system of qubits. For single qubit manipulations these transformations acted on a 2 dimensional space. Our Bloch sphere analysis of a general qubit allowed us

to find all the operations we needed. However, extending the Bloch sphere to multiple qubits is impossible. When we start talking about a larger number of qubits, the dimensionality of the system grows. The dimension of the system is related to the total number of states realizable. For 2 qubits there are four possible basis states {00,01,10,11}. The dimensionality grows as $2^{\#qubits}$ so that 500 qubits constitutes a number of states larger than the hypothesized number of atoms in the universe! Clearly depicting such a space intuitively is impossible.

As a guide we shall therefore begin with our classical knowledge of logic gates. The NOT gate is the only classic gate which acts on a single bit, and as we already showed, this operation is possible with Pauli rotations. The other common logic gates are the OR, AND, XOR, NOR, and NAND gates and they all act on 2 input bits and produce a single output bit. These gates are defined by their truth tables which show all the possible input states and corresponding output states. The most important of these gates are the NAND and the NOR gates as it can be proven all possible logic operations can be reduced to a series of either NAND or NOR gates. That is to say that the NAND or the NOR gate is a classical universal gate for classical computation. The NAND truth table is shown in Table 1.4.1.

a	b	NOT(a AND b)
0	0	1
0	1	1
1	0	1
1	1	0

TABLE 1.4.1. NAND Truth Table

These gates are placed in logic circuits for complex logic analysis. These classical circuits have a number of properties. First is the *fanout/fan-in* property, whereby splitting a wire carrying a bit signal we can instantly create a copy of that bit or combining two wires into one we can perform an AND operation. A fanout of the input bit before a NAND gate makes it a NOT gate since (a NAND a) = (NOT a) as you can see in the last row of the truth table. *Ancilla* bits are also allowed, in which one of the input bits, is set to a particular value in order to more precisely define the operation of the gate. Bits can be interchanged via a crossover of the wires, this is identical to a swap operation in which the value of two bits are swapped. And finally, we notice that the number of input bits does not equal the number of output bits.

If we now try to find equivalent quantum gates we run into some problems. First off, as stated previously, but yet to be proven, qubits can not be copied. That is quantum circuits can not fanout/fan-in. There is nothing suggesting Ancilla bits are not allowed, since we do have the ability to initialize qubits. We should also be able to crossover/swap qubits without any physical limitation. However, due to the second postulate of quantum mechanics the evolution, or transformation, of a quantum system must be unitary. This means that the transformation U must satisfy $U^*U = UU^* = I$ where I is an identity matrix. Since our gates are transformations on the system and they must be unitary it means they must be reversible. Classical gates are not reversible since the output can not always be determined from the input. For the NAND gate, if the output is zero we do not know the state of the bits before the gate with certainty. This is largely due to the fact that the number of input bits may be larger than the number of output bits. This will not be possible for our quantum gates.

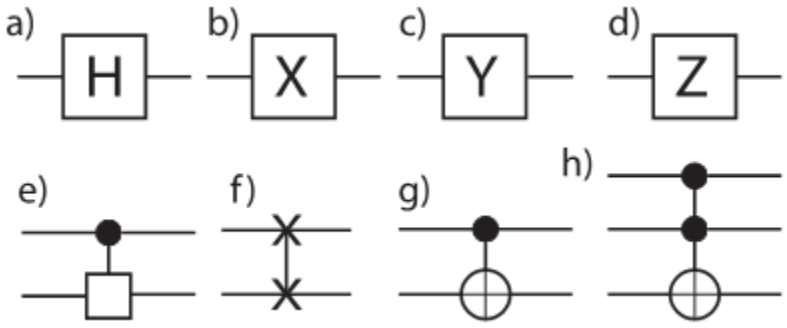

FIGURE 1.4.1. Circuit diagram representation of various quantum gates. a) Hadamard b) Pauli X c) Pauli Y d) Pauli Z e) Controlled gate, the solid dot represents the control qubit f) SWAP gate g) CNOT h) Toffoli (CCNOT)

This may make you wonder if quantum gates can do everything classical gates can do. That is to say is there an equivalent classical universal gate like the NAND gate which is a quantum gate. The answer to this is yes, and there are a couple of quantum gates which allow for universal classical computation, one of which is the Toffoli gate or the controlled controlled not gate (CCNOT). Before we describe it we will start with a simple Swap gate.

The quantum Swap gate is probably the simplest operation one can imagine with two qubits. The swap operation simply interchanges the states of two qubits a, b. The easiest way define the gate is with a truth table, however we must remember that when we talk about the composite state of the system, the fourth postulate of quantum mechanics tells us that we must take the tensor product of the two constituent states to make the full state. That is the quantum state of both qubits being in the zero state, written $|00\rangle = |0\rangle \otimes |0\rangle$. Using again $|0\rangle = \begin{pmatrix} 0 \\ 1 \end{pmatrix}$ and $|1\rangle = \begin{pmatrix} 1 \\ 0 \end{pmatrix}$, our truth table would look something like

$$|00\rangle \to |00\rangle = \begin{pmatrix} 0 \\ 0 \\ 0 \\ 1 \end{pmatrix} \to \begin{pmatrix} 0 \\ 0 \\ 0 \\ 1 \end{pmatrix} \qquad |01\rangle \to |10\rangle = \begin{pmatrix} 0 \\ 0 \\ 1 \\ 0 \end{pmatrix} \to \begin{pmatrix} 0 \\ 1 \\ 0 \\ 0 \end{pmatrix}$$

$$|10\rangle \to |01\rangle = \begin{pmatrix} 0 \\ 1 \\ 0 \\ 0 \end{pmatrix} \to \begin{pmatrix} 0 \\ 0 \\ 1 \\ 0 \end{pmatrix} \qquad |11\rangle \to |11\rangle = \begin{pmatrix} 1 \\ 0 \\ 0 \\ 0 \end{pmatrix} \to \begin{pmatrix} 1 \\ 0 \\ 0 \\ 0 \end{pmatrix}$$

Our matrix equation for our transformation will look like $U_{trans} M_{input} = M_{output}$ where M is a matrix composed by the constituent column vectors of possible input/output states in identical order. Solving for U_{swap} we get

$$U_{swap} \begin{bmatrix} 0 & 0 & 0 & 1 \\ 0 & 0 & 1 & 0 \\ 0 & 1 & 0 & 0 \\ 1 & 0 & 0 & 0 \end{bmatrix} = \begin{bmatrix} 0 & 0 & 0 & 1 \\ 0 & 1 & 0 & 0 \\ 0 & 0 & 1 & 0 \\ 1 & 0 & 0 & 0 \end{bmatrix} \to \underline{U_{swap} = \begin{bmatrix} 1 & 0 & 0 & 0 \\ 0 & 0 & 1 & 0 \\ 0 & 1 & 0 & 0 \\ 0 & 0 & 0 & 1 \end{bmatrix}}$$

As we can see the swap operator is Hermitian and unitary as expected.

There are a group of quantum gates called control gates. A control gate, such as the controlled NOT gate (CNOT) performs a logic operation "if and only if, then". That is a control gate has an input qubit, the control bit, which controls if a particular operation will or will not occur on a target qubit. The truth table and subsequent matrix representation for a CNOT gate will therefore look like that in Table 1.4.2. This can be understood as "if and only if the control qubit a is 1, then NOT qubit b.

$\|ab\rangle$	CNOT($\|ab\rangle$)
$\|00\rangle$	$\|00\rangle$
$\|01\rangle$	$\|01\rangle$
$\|10\rangle$	$\|11\rangle$
$\|11\rangle$	$\|10\rangle$

$$U_{CNOT} = \begin{bmatrix} 1 & 0 & 0 & 0 \\ 0 & 1 & 0 & 0 \\ 0 & 0 & 0 & 1 \\ 0 & 0 & 1 & 0 \end{bmatrix}$$

TABLE 1.4.2. CNOT Truth Table and Matrix

Finally, we have the CCNOT gate, or the Toffoli gate which, as stated previously, is a universal gate for *classical* computations. That is, with this gate all classical logic operations can be performed. The gate has 2 control qubits, a and b and one target qubit, c. The matrix representation for this 8x8 square matrix is the direct sum of a 6x6 identity matrix and the the Pauli X gate. The gate simply NOTs the target qubit if and only if both the control qubits are 1. Mathematically and concisely we can say it maps the state $|a, b, c\rangle$ to $|a, b, c \oplus a * b\rangle$ where $\oplus$ defines Boolean addition and $*$ defines algebraic multiplication.

The question you may be wondering now is, is there a universal quantum gate, or set of quantum gates which can perform any and all *quantum* operations? It turns out there are and it can be shown that all quantum operations can be broken down into series of single qubit rotations and CNOT gates. The math and proofs are beyond this course, but an accepted universal set of quantum gates can be shown to be the Hadamard gate, the $R_Z(\pi/4)$ and the CNOT gate. These will not always produce the most efficient set of gates to perform a particular operation, but it can reproduce any operation with reasonable efficiency.

With all of this we now have a guide for what to look for in a physical implementation for quantum computing. Specifically, we need to find a system with Pauli operators present which hopefully we can

control. We also need a physical implementation for a CNOT gate such that if one qubit is in the excited state it will cause the other qubit to change states. Finally, implementing a functional Toffoli gate will complete the system so that all quantum and classical logical operations can be accomplished. All of this was found just from considering general QIS arguments and following the DiVincenzo criteria as well as the quantum postulates.

1.5. Measurement and Entanglement

The nature of what constitutes a "measurement" and the "collapse" of a quantum state has been a convoluted and intensely debated topic since the development of quantum mechanics. For the purposes of this course, we are going to side step this conversation and simply define a measurement to be the intended consequence of interacting a closed quantum system, our qubits, with an external system in a controlled manner, from which some information about the quantum state of the qubits can be recovered. A device which performs a "measurement" should ideally be able to be turned "on" and "off" to control when a measurement occurs. It should, with high fidelity, be able to map the state of the qubit to a state of measurement outcomes. And the measurement apparatus should perform the measurement quickly compared to the coherence time of the qubit.

Mathematically, measurement is defined by a set of operators $\{\mathcal{M}_m\}$ which act on the state space of the system. The probability of a measurement result m occurring when the state Ψ is measured upon is

$$P(m) = \langle\Psi| \mathcal{M}_m^\dagger \mathcal{M}_m |\Psi\rangle \tag{1.5.1}$$

The state of the system after the measurement is

$$|\Psi'\rangle = \frac{\mathcal{M}_m |\Psi\rangle}{\sqrt{P(m)}} \tag{1.5.2}$$

and the sum of probabilities of all possible measurement outcomes should be complete, i.e.

$$\sum_m P(m) = \sum_m \langle\Psi| \mathcal{M}_m^\dagger \mathcal{M}_m |\Psi\rangle = 1 \tag{1.5.3}$$

This also implies $\sum_m \mathcal{M}_m^\dagger \mathcal{M}_m = I$ where I is the identity matrix. Intuitively these arguments should make sense. The first equation is simply the general probabilistic interpretation of the wave equation of general quantum mechanics. The second equation is a consequence of the fact that all measurements will ever reveal are eigenstates of the measurement operator which acts on the system. While the final equation simply implies that if we add all the possible probabilities of all possible measurement outcomes, we should get everything! This is also a classical statistical argument.

There are an infinite set of possible measurement operators, as any set which satisfy the above 3 equations is a valid set of quantum measurements, however one of the simplest examples is probably the measurement operators defined by

$$\mathcal{M}_0 = |0\rangle\langle 0| = \begin{bmatrix} 0 & 0 \\ 0 & 1 \end{bmatrix} \qquad \mathcal{M}_1 = |1\rangle\langle 1| = \begin{bmatrix} 1 & 0 \\ 0 & 0 \end{bmatrix}$$

When these operators act on the general state $|\Psi\rangle = \alpha|0\rangle + \beta|1\rangle$ we get

$$P_0 = \langle\Psi| \mathcal{M}_0^\dagger \mathcal{M}_0 |\Psi\rangle = \begin{bmatrix} \beta & \alpha \end{bmatrix} \begin{bmatrix} 0 & 0 \\ 0 & 1 \end{bmatrix} \begin{bmatrix} 0 & 0 \\ 0 & 1 \end{bmatrix} \begin{bmatrix} \beta \\ \alpha \end{bmatrix} = |\alpha|^2$$

$$P_1 = \langle\Psi| \mathcal{M}_1^\dagger \mathcal{M}_1 |\Psi\rangle = \begin{bmatrix} \beta & \alpha \end{bmatrix} \begin{bmatrix} 1 & 0 \\ 0 & 0 \end{bmatrix} \begin{bmatrix} 1 & 0 \\ 0 & 0 \end{bmatrix} \begin{bmatrix} \beta \\ \alpha \end{bmatrix} = |\beta|^2$$

These are computational projection measurements which measure if the system is in state 0 or 1 and mathematically tell us the probability of each possibility. Effectively it projects the qubit vector onto the z-axis of the Bloch sphere. However, if we want to actually measure the value of α and β we need to prepare and measure $|\Psi\rangle$ an infinite number of times since the measurement outcome m will only ever be 0 or 1. In order to have full knowledge of a general state $|\Psi\rangle$ we need to know α and β. With a single measurement it is impossible to do this so we are extremely limited in how much information we can get out of a qubit. This has far reaching consequences which are amplified by the no-cloning theorem which will be discussed in the next section.

After such a measurement the state of the system becomes

$$|\psi_0\rangle = \frac{\mathcal{M}_0 |\Psi\rangle}{\sqrt{P_0}} = \frac{\alpha}{|\alpha|} |0\rangle \qquad |\psi_1\rangle = \frac{\mathcal{M}_1 |\Psi\rangle}{\sqrt{P_1}} = \frac{\beta}{|\beta|} |1\rangle$$

and here we more clearly see the projection of the vector into one of the basis states. If we repeat another measurement after the initial one, assuming zero energy loss, we find that

$$P_{00} = 1 \qquad P_{11} = 1$$
$$P_{01} = 0 \qquad P_{10} = 0$$

This probability outcome, as regarded by the Copenhagen interpretation of quantum mechanics, is the "collapse" of the wave function onto one of the basis states. That is all cross terms and any superposition appears to vanish.

In practice however, a repeat measurement may not always reproduce the same result. The interaction between the measuring apparatus and the quantum system may actually cause a physical change in the state of the system. For example, a photo-detector often absorbs the photon it is trying to measure, at which point attempting to remeasure the photon is impossible. Measuring the position of a particle often causes you to move the particle, thereby causing a repeat measurement not to produce an identical result. A measurement is said to be Quantum Non-Demolition if repeated measurements reproduce identical results. This can occur if the observable commutes with the complete Hamiltonian of the qubit and the measuring apparatus system. This however does not mean there is no back-action on the quantum system during the measurement process. Typically, a QND measurement allows for repeated measurement of one type of observable with the cost of losing complete knowledge of another type of observable of the system, such as the phase. As a qualitative example, using a mirror attached to a spring as a measuring device can couple the reflection, and therefore presence of the photon, to oscillations in the spring. This way the photon is not completely destroyed, though its state may be altered by the reflection in most cases. Nevertheless, QND is thus something a physical system should strive to achieve when measuring the states of qubits.

Of course there are other possibilities for why repeated measurements do not produce identical results. Specifically, relaxation, decoherenece and other forms of energy loss and natural evolution of a system may cause differences in repeat measurements. Great care must be taken to design systems to minimize these effects, or get around them by performing tasks relatively faster than these effects will noticeably change the system.

There are unique quantum states called entangled states which have interesting measurement results. An entangled state is a composite state of two or more systems which can not be written as a tensor product of the original component systems. That is to say $|\Psi_{1,2\,\text{entangled}}\rangle \neq |\Psi_{1,2}\rangle = |\Psi_1\rangle \otimes |\Psi_2\rangle$. For example take the state

$$|\Psi_{\text{entangled}}\rangle = \frac{1}{\sqrt{2}} (|00\rangle + |11\rangle)$$

if we attempt to write this as a product of two states $|\psi_1\rangle = \alpha |0\rangle + \beta |1\rangle$ and $|\psi_2\rangle = \gamma |0\rangle + \delta |1\rangle$we find $|\Psi_{12}\rangle = \alpha\gamma |00\rangle + \alpha\delta |01\rangle + \beta\gamma |10\rangle + \beta\delta |11\rangle$. In order for $|\Psi_{\text{entangled}}\rangle$ to equal $|\Psi_{12}\rangle$ then $\alpha\gamma = \beta\delta = \frac{1}{\sqrt{2}}$ and $\alpha\delta = \beta\gamma = 0$ must be satisfied. However, there is no solution for any complex values α, β, γ or δ.

One way to create this state is to perform a Hadamard gate on a 0 qubit and then use that as a control bit for a CNOT gate with another 0 qubit as follows.

$$|\Psi_1\rangle = U_{\text{Had}} |0\rangle = \frac{1}{\sqrt{2}} (|0\rangle + |1\rangle)$$
$$|\Psi_{12}\rangle = |\Psi_1\rangle \otimes |\Psi_2\rangle = \frac{1}{\sqrt{2}} (|0\rangle + |1\rangle) \otimes |0\rangle = \frac{1}{\sqrt{2}} (|00\rangle + |10\rangle)$$
$$|\Psi_{\text{entangled}}\rangle = U_{\text{CNOT}} |\Psi_{12}\rangle = \frac{1}{\sqrt{2}} (|00\rangle + |11\rangle)$$

This procedure will also work with the two qubits in the other possible combinations of computational input state. The results are the 4 maximally entangled states called Bell states given the names below

$$\begin{aligned}
\left|\Phi^+\right\rangle &= \frac{1}{\sqrt{2}}\left(|00\rangle + |11\rangle\right) \\
\left|\Phi^-\right\rangle &= \frac{1}{\sqrt{2}}\left(|00\rangle - |11\rangle\right) \\
\left|\Psi^+\right\rangle &= \frac{1}{\sqrt{2}}\left(|01\rangle + |10\rangle\right) \\
\left|\Psi^-\right\rangle &= \frac{1}{\sqrt{2}}\left(|01\rangle - |10\rangle\right)
\end{aligned} \tag{1.5.4}$$

The most interesting property of such a state is the measurement correlations between the two qubits. If we use our measurement operators from before on the individual qubits we find

$$P_{0,\,\text{first}} = \langle\Psi_{\text{entangled}}|\left(\mathcal{M}_0 \otimes I\right)^\dagger\left(\mathcal{M}_0 \otimes I\right)|\Psi_{\text{entangled}}\rangle = \frac{1}{2}$$

where $P_{0,\,\text{first}}$ denotes the probability of measuring the first qubit in the ground state 0. $(\mathcal{M}_0 \otimes I)$ is a mathematically concise and correct way to apply the measurement operator on only the *first* qubit. After this measurement the new state of the system will be

$$|\Psi_{\text{post}}\rangle = \frac{\left(\mathcal{M}_0 \otimes I\right)|\Psi_{\text{entangled}}\rangle}{\sqrt{P_{0,\,\text{first}}}} = |00\rangle$$

now if we measure the second qubit to see if it is in the ground state we find

$$P_{0,\,\text{second}} = \langle\Psi_{\text{post}}|\left(I \otimes \mathcal{M}_0\right)^\dagger\left(I \otimes \mathcal{M}_0\right)|\Psi_{\text{post}}\rangle = 1$$

where $(I \otimes \mathcal{M}_0)$ is the mathematically concise and correct way to apply the measurement operator on the second qubit. The results of this shows that when we measure the first qubit we have a 50/50 chance of finding it in the ground state. If we do find it in the ground state we know with unit certainty that the second qubit is also in the ground state. If we repeated all the possible measurements we find that the measurement outcomes between the two qubits are always and completely correlated. Such correlations are stronger than any classically possible correlations and are therefore a new tool we can use in quantum calculations which is unavailable to classical computations. These entangled states have been used in quantum teleportation, superdense coding and other interesting protocols in QIS.

These entangled states are at the heart of the great controversy and reluctance for many scientist of the past to grip the realities of quantum mechanics. A paper written by Einstein and others lead to the EPR paradox in which it was postulated that quantum mechanics must be incomplete since such states threaten local causality. However, in 1964 Bell wrote his famous paper outlining the inconsistency of quantum mechanics with any locally real based hidden variable theory. Bell postulated his famous inequalities in which the quantum mechanical correlations of entangled states could not be explained classically and gave experimental predictions which could test if quantum mechanics was complete and correct. The four bell states in equation 1.5.4 are called maximally entangled states because the correlations between the two qubits have the greatest possible value. Specifically, in a theory built upon Bell's original ideas it can be show that a hidden variable, locally realistic theory of quantum mechanics will predict a maximum correlation of outcomes of 2. However, quantum mechanics, as it is, predicts a $2\sqrt{2}$ correlation between the outcomes of these states. Since this paper, numerous experiments have been conducted testing this theory and the overwhelming evidence is in favor of Quantum Mechanics, as it is, being complete and correct.

Luckily for Einstein, perhaps not for us, there has been no way to utilize these entangled states which allows for faster than light communication. Indeed, though the information between the two entangled qubits appears to transmit instantaneously, the outcome of the first measurement can not be controlled, nor is there anyway to know if the other qubit has been measured in a faster than light manner.

An analogy for this would be something like having two playing cards, an ace of spades and an ace of diamonds. A dealer shuffles the cards and places them face down on the table. A person named Alice takes one of the cards and goes across the room without looking at the card, while a person named Bob holds on to the other card. Now from Bob's perspective, before he flips his card over all he can say is that there is a 50% chance he will have the ace of spades and a 50% chance he has the ace of diamonds. Once he flips his

card over and makes a "measurement" he determines his card is the ace of spades and immediately knows that Alice is holding the ace of diamonds. However, even if Bob has "measured" his card, Alice will still know nothing about her card beyond that 50/50 chance. She can, however know what it is before measuring it if Bob yells across the room and says he has the ace of spades. However, this form of communication is classical and is limited to the speed of light. Also, because Bob does not control the shuffling of the cards, there is no way for him to communicate a message to Alice faster than light.

This may seem to make this entanglement rather mundane, but the place the analogy breaks down and where entanglement really is interesting is when an entangled state of two qubits interacts with a third. This is what is used in the teleportation protocol which will be explained in the next section.

1.6. Energy Relaxation, τ_1, and Coherence τ_2

The final term to discuss in the DiVincenzo criteria is the coherence time. Typically, there are two parameters which characterize the stability of a qubit τ_1 and τ_2.

τ_1 has many names including the "longitudinal coherence time", the "spontaneous emission time", the "relaxation time" and many others. Qubits are physically two level quantum systems which, when in the excited state, will naturally decay to the thermal equilibrium ground state. This spontaneous decay is related to the the quantum system interacting and mixing with its environment, so that each type of qubit will have its own unique relaxation time. In order to determine the time τ_1 a simple experiment can be performed in which a π pulse is applied to the qubit about an axis on the equator of the Bloch sphere, i.e. the qubit is brought into the excited state. After the pulse is applied there is a time delay, $\triangle t$, before a measurement of the qubit is performed. By performing many such experiments averaging the results and varying the time delay, a characteristic exponential decay $\propto e^{-\triangle t/\tau_1}$ will be recovered, from which τ_1 can be extracted. The exact measurement techniques will vary between physical systems due to the nature of the physical system and a desire for QND measurements and reduction of errors, however the principle and characteristic of the relaxation time is always the same.

The τ_2 time also has many names including the "transverse coherence time", "phase damping time", "spin-spin relaxation time" and many others. Ultimately, this term relates to how long we can control the phase term of the qubit. The exact mechanisms which causes rotations of the qubit vector around the z-axis, i.e controls the phase, are unique to the physical system, as we shall see in the rest of this script. However, in general, the qubit mixing with the environment will cause fluctuations in our expected rate of rotation.

A simple experiment measuring so called Ramsey Fringes will determine τ_2. The experiment is similar to the experiment for τ_1 except this time instead of a single π pulse we use two $\pi/2$ pulses separated by a delay time. Specifically, the experiment starts with a $\pi/2$ rotation about the y-axis to bring the qubit to the x-axis in an equal superposition. Then the qubit is left alone for a time $\triangle t$ and will naturally precess around the z-axis. After this time a final $\pi/2$ rotation is performed around the y-axis and is subsequently measured. Performing many such experiments averaging and varying the delay time $\triangle t$ will produce a dampened sinusoidal function which oscillates about 0.5 with some characteristic frequency. The exponentially decaying envelope will be proportional to $e^{-\triangle t/\tau_\varphi}$.

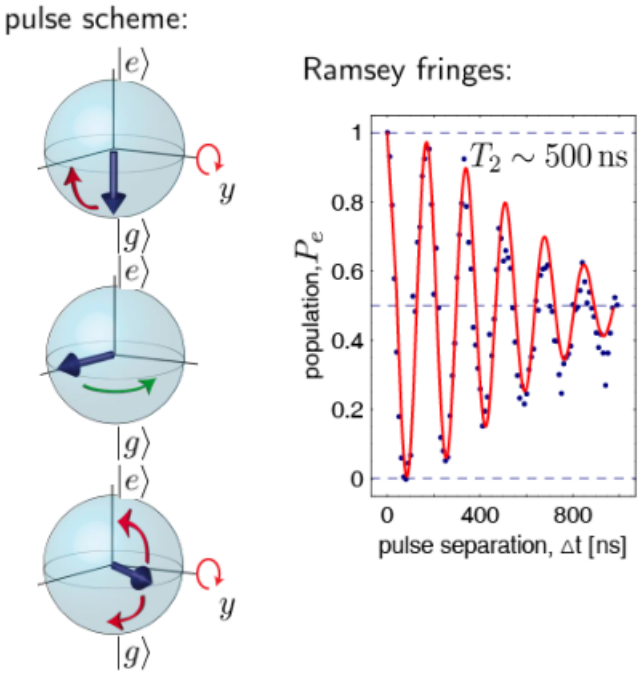

FIGURE 1.6.1. Ramsey Fringe experiment to determine the transverse coherence time.

Finally we can use the equation

$$\frac{1}{\tau_2} = \frac{1}{2\tau_1} + \frac{1}{\tau_\varphi}$$

to determine τ_2.

In general both of these processes relate to energy loss and the decay of the Bloch vector components. In nearly all situations $\tau_1 \geq \tau_2$ so that the most important stability parameter is τ_2 and this represents the generic "coherence time" of the qubit.

1.7. The No Cloning Theorem and Quantum Teleportation

Before we get into quantum teleportation we will finally prove the No Cloning Theorem which has been referenced already a couple of times. Cloning classically is a very simple concept and used in numerous communication protocols for error correction. A simple fan-out in a circuit is a classical cloning machine in which the input of a classical bit becomes two outputted and identical bits. Let's see if such an operation is possible quantum mechanically.

Suppose we have a general unknown qubit, "A", in state $|\Psi_A\rangle = \alpha|0\rangle + \beta|1\rangle$. We wish to put this through a copying gate which will produce the original qubit A and an identical qubit B. Assuming qubit B starts in the $|0\rangle$ state we mathematically wish to have

$$U_{\text{copy}}|\Psi_A\rangle|0_B\rangle = |\Psi_A\rangle|\Psi_{B=A}\rangle$$
$$|\Psi_A\rangle|\Psi_{B=A}\rangle = (\alpha|0\rangle + \beta|1\rangle)^2 = \alpha^2|00\rangle + \alpha\beta|01\rangle + \beta\alpha|10\rangle + \beta^2|11\rangle$$

Nothing wrong so far. U_{copy} should work if $|\Psi_A\rangle$ is in a pure basis state as well that is $|\Psi_A\rangle = |0\rangle$ or $|\Psi_A\rangle = |1\rangle$ so that

$$U_{\text{copy}}|0_A\rangle|0_B\rangle = |0_A\rangle|0_B\rangle$$
$$U_{\text{copy}}|1_A\rangle|0_B\rangle = |1_A\rangle|1_B\rangle$$

Since U_{copy} in a linear operator we can expand Ψ_A before applying the operator and find

$$U_{\text{copy}}|\Psi_A\rangle|0_B\rangle = U_{\text{copy}}(\alpha|0\rangle + \beta|1\rangle)|0_B\rangle = \alpha|0_A\rangle|0_B\rangle + \beta|1_A\rangle|1_B\rangle$$

which is not consistent with our original result $\alpha^2|00\rangle + \alpha\beta|01\rangle + \beta\alpha|10\rangle + \beta^2|11\rangle$. This means that a general qubit state can not be copied. If the qubit we wish to copy is in a basis state, it can be copied, that is if $\alpha = 1 \wedge \beta = 0$ or $\beta = 1 \wedge \alpha = 0$ where $\wedge$ is a logical "AND" then we are fine. However, if the qubit is in a general superposition state, we can not copy it.

You may be wondering why we can not just measure qubit A and then initialize both qubits in that state. However, you are forgetting that a single measurement of a qubit does not reveal the values of α and β only the basis state it will be in now. Since we can not determine exactly α and β without a large number of measurement results on identically prepared qubits and we originally do not know the value of α and β of the qubit we wish to copy, we can not prepare the necessary qubits for measurement and subsequent copying! This is very much a qualitative restatement of the No-Cloning theorem.

There is much to be said about this theorem. First it can be seen as an indirect result of the uncertainty principle of quantum mechanics. If we could clone unknown quantum states, then we could measure the attributes of such a state/system with infinite precision, thus violating the uncertainty principle. This theorem also prevents superluminal communication using entangled states of qubits. Though, it does not prevent superluminal communication in general, but only for this particular case. Quantum Cryptography is very much based on the validity of this theorem since it will prevent the man-in the middle attack where the eavesdropper will no longer be able to "copy" the key for himself and then allow it to continue down the communication line. As previously stated, this does not allow for classical forms of error correcting, where typically a bit is copied multiple times and each is used in identical operations and the majority outcome is taken as the result. Finally, it should be noted that it is possible to imperfectly clone unknown quantum states with various limitations and constraints. Imperfect cloning does have applications including possibilities for quantum man in the middle attacks. Also, this theorem does not prevent quantum error correction, it simply requires non-classical engineering to do and in 1995 Shor and Steane created the first quantum error correcting algorithms which circumvent the problems caused by this theorem.

Now that we have finally proved the no-cloning theorem, we might wonder how to get the information stored in a qubit at location A, to another location, B. The no-cloning theorem does not allow us to clone the

qubit at point A to get all the needed information about its state and relay that to location B to initialize a qubit there. For that matter, how will we ever be able to share quantum information in a network? Just about everything we would try classically will not work! In 1993 a solution by C. Bennet and colleagues was developed in which maximally entangled qubits could be used along with some classical information to effectively "teleport" the unknown state of a qubit between two locations.

Before we describe the procedure, I would like to go back to the analogy previously stated regarding quantum entanglement. I stated that an interesting aspect of entanglement was the correlated outcomes of measurement results between two qubits separated by an arbitrary distance. I also stated that this was similar to the measurement results of having two playing cards shuffled face down and measuring the first one. The analogy breaks down, however, in that classically, we know that the cards where their original values before we flipped them over, and it was simply our inability to follow the shuffling that did not allow us to predict with certainty the result of flipping the first card. Quantum mechanically speaking we have to abandon this idea, or at least the idea of local realism, to interpret this entanglement. Specifically, we must abandon the notion that the cards had their values before they were flipped as we will see why in a moment.

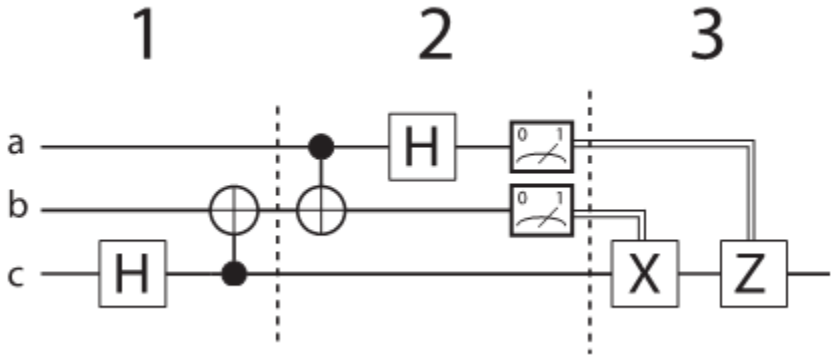

FIGURE 1.7.1. Teleportation Protocol Circuit Diagram. Part 1 creates the entanglement of the messenger qubit, b, with the receiver qubit c. Part 2 is the interaction of the messenger qubit and the transmission qubit, a, and full state measurements of the two qubits afterward. Part 3 is the classical transfer of information about the measured state of qubits a and b with the conditional Pauli gates to act on qubit c if the corresponding qubit was found in the excited state.

In the standard quantum teleportation protocol we would like to transmit qubit a at location A to location B. To perform the operation we need three qubits, a, the "transmission" qubit , qubit b the "messenger" and qubit c the "receiver" qubit. First, qubits b and c are maximally entangled and qubit b is sent to location A while qubit c is sent to location B. At location A we perform a CNOT(a, b) followed by a Hadamard gate on a. After, a projection measurement on both qubit a and b is performed collapsing their states. When this happens, information about qubit a is "teleported" to qubit c. At this point the results of the measurements at location A must be relayed to location B, where then qubit c can be rotated appropriately to reconstruct c into a. In the process qubit a is destroyed, so that a copy has not been created, thereby circumventing the no-cloning theorem. It should be noted that qubit b never physically leaves location A and for all practical definitions "teleports" information about qubit a to qubit c.

Let's look at the math to better understand this. Qubit a, the qubit with the information we wish to send is in the unknown state $|\Psi_a\rangle = \alpha|0_a\rangle + \beta|1_a\rangle$ while qubit b and c are prepared in the Bell state $\frac{1}{\sqrt{2}}(|0_b0_c\rangle + |1_b1_c\rangle)$. The entire system is therefore in the state

$$|\Psi_\Sigma\rangle = |\Psi_a\rangle|\Psi_{bc}\rangle = \frac{1}{\sqrt{2}}(\alpha|000\rangle + \alpha|011\rangle + \beta|100\rangle + \beta|111\rangle)$$

where $|abc\rangle$ represents the composite basis state of qubit a, b and c respectively. When we apply the CNOT to the first two qubits, we flip qubit b if a is 1 so we get

$$U_{\mathrm{CNOT}(a,b)} \left|\Psi_{\sum}\right\rangle = \frac{1}{\sqrt{2}} \left(\alpha \left|000\right\rangle + \alpha \left|011\right\rangle + \beta \left|110\right\rangle + \beta \left|101\right\rangle\right)$$

then we apply the Hadamard to a so that $|0_a\rangle \to \frac{1}{\sqrt{2}} \left(|0_a\rangle + |1_a\rangle\right)$ and $|1_a\rangle \to \frac{1}{\sqrt{2}} \left(|0_a\rangle - |1_a\rangle\right)$ and the system becomes

$$\begin{aligned} U_{\mathrm{Had(a)}} U_{\mathrm{CNOT(a,b)}} \left|\Psi_{\sum}\right\rangle = \frac{1}{2} \left(\alpha \left|000\right\rangle + \alpha \left|100\right\rangle + \alpha \left|011\right\rangle + \alpha \left|111\right\rangle \right. \\ \left. + \beta \left|010\right\rangle - \beta \left|110\right\rangle + \beta \left|001\right\rangle - \beta \left|101\right\rangle\right) \end{aligned}$$

we can rewrite this in a more suggestive form based on the four possible measurement outcomes of qubits a and b. Specifically,

$$U_{\mathrm{Had(a)}} U_{\mathrm{CNOT(a,b)}} \left|\Psi_{\sum}\right\rangle = \frac{1}{2} \begin{bmatrix} \left\{ \begin{array}{ll} |0_a 0_b\rangle \left(\alpha \left|0_c\right\rangle + \beta \left|1_c\right\rangle\right) & + \\ |1_a 0_b\rangle \left(\alpha \left|0_c\right\rangle - \beta \left|1_c\right\rangle\right) & + \\ |0_a 1_b\rangle \left(\beta \left|0_c\right\rangle + \alpha \left|1_c\right\rangle\right) & + \\ |1_a 1_b\rangle \left(\beta \left|0_c\right\rangle - \alpha \left|1_c\right\rangle\right) & \end{array} \right. \end{bmatrix}$$

We can notice that now $|\Psi_c\rangle$ which are the states in parenthesis look nearly identical to $|\Psi_a\rangle$, but sometimes rotated or flipped. We could rewrite this as

$$\left|\Psi_{\mathrm{Teleport}}\right\rangle = U_{\mathrm{Had(a)}} U_{\mathrm{CNOT(a,b)}} \left|\Psi_{\sum}\right\rangle = \frac{1}{2} \begin{bmatrix} \left\{ \begin{array}{ll} |0_a 0_b\rangle \hat{\sigma}_I \left|\Psi_{c=a}\right\rangle & + \\ |1_a 0_b\rangle \hat{\sigma}_Z \left|\Psi_{c=a}\right\rangle & + \\ |0_a 1_b\rangle \hat{\sigma}_X \left|\Psi_{c=a}\right\rangle & + \\ |1_a 1_b\rangle \hat{\sigma}_{XZ} \left|\Psi_{c=a}\right\rangle & \end{array} \right. \end{bmatrix}$$

and we see clearly that the state of qubit c depends on the measurement outcome of a and b and is different from the original state of a by a rotation or two. Once the measurement of qubits a and b is made at location A, this information is relayed to location B classically, and then the necessary rotations to change qubit c into the original state of qubit a can be performed. Thereby teleporting the information between the two locations.

Now the place where the card analogy breaks down is that the playing cards do not interact with each other. That is to say, if we put a third card next to one of the original face down cards, it would not cause that card to change nor the card on the other side of the room to change as well. However, this is what actually happens with quantum systems. It is as if there is a quantum channel of information connecting the entangled qubits which allows the transmission of information between them and causes "spooky action at a distance". Unfortunately, this quantum channel, for the time being, seems to be outside of our ability to control exactly how the transfer of our desired information will happen. However, we can clearly utilize it for transferring quantum information from one location to another, with the help of some means of classical communication.

The term teleportation used in this context is from that fact that information about qubit a is transmitted to qubit c through qubit b, without qubit b going back to the location of qubit c and that qubit c and qubit a never directly interact. It is not necessarily the same concept of teleportation in Sci-Fi where matter is relocated from one place to another. However, it is without a doubt similar in character. Possibly in the future, entanglement and a deeper understanding of this hidden quantum channel might remove some of the mystery of such a teleportation, but until then, this is probably an adequate use of the term.

1.8. Summary

We have now covered all the basics of what we need to cover from general QIS to begin looking for physical systems which can realize full and general quantum information processing. The rest of this course will cover the various fields of physical systems which have already been able to realize some or even all of what we have previously talked about. These systems include Nuclear Magnetic Resonance, photon based systems, superconducting circuits, trapped ions and quantum dots. Superconducting circuits will be used as the example physical system for going into greater detail about how these general qubits are created, how qubit manipulation and gates are implemented as well as how measurements are performed. This is done

simply because most of the fields have a large overlap in details such that studying one of them in detail actually gives you a lot of knowledge and skills easily transferable to the other fields. Also, there is not enough time in one course to cover extensively each field as each field could easily warrant its own unique course.

CHAPTER 2

Superconducting Circuits

2.1. The Harmonic Oscillating Circuit

How can we make a circuit which can be used for quantum information processing? If we recall from any basic Electromagnetism course the parallel LRC circuit will act in many ways like a mechanical harmonic oscillator. We also know from basic quantum mechanics that the mechanical harmonic oscillator will have quantized energy levels. This suggests that an LRC circuit might be able to be used for quantum information processing. However, we need to figure out if the electric circuit will also quantize as the mechanical system does and determine the relevant parameters of the system.

Our analysis starts with what we know classically about the circuit. For simplicity we will ignore the resistor and consider its effects on the system afterward. Thus, the basic LC circuit is drawn in Figure 2.1.1. The basic circuit equations are

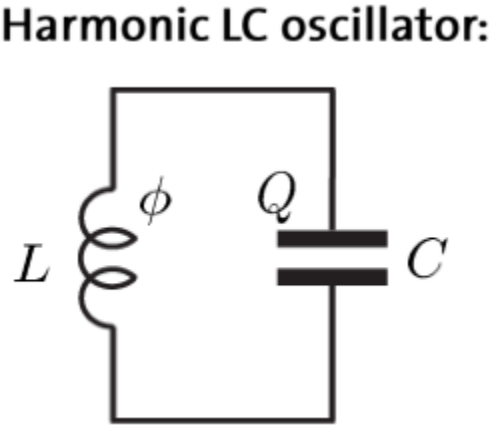

FIGURE 2.1.1. A simple LC circuit

$$\Phi = LI \qquad V_L = -L\frac{dI}{dt} \tag{2.1.1}$$

$$Q = CV_C \tag{2.1.2}$$

$$E_{\text{mag}} = \frac{LI^2}{2} \qquad E_{\text{elec}} = \frac{CV^2}{2} \tag{2.1.3}$$

where Φ is the magnetic flux in the inductor, L the inductance, I the current, and Q the total charge on the capacitor. Also, C is the capacitance, $V_{\text{L,C}}$ the voltage across the inductor/capacitor and $E_{\text{mag,elec}}$ is the energy stored in the inductor and capacitor respectively.

We can write the classic Hamiltonian as

$$H_{\text{cl,LC}} = \frac{CV^2}{2} + \frac{LI^2}{2} = \frac{Q^2}{2C} + \frac{\Phi^2}{2L} \tag{2.1.4}$$

where we have chosen to write the Hamiltonian in terms of the charge and magnetic flux.

Now we are stuck since we do not know the quantum operators for Q and Φ. For inspiration, let us turn to the mechanical harmonic oscillator. Recall the Hamiltonian for the classic mechanical harmonic oscillator, for example a mass on a spring, is

$$H_{\text{cl,mech}} = \frac{p^2}{2m} + \frac{kx^2}{2} \tag{2.1.5}$$

where p is the momentum of the mass m, k the spring constant and x is the displacement of the mass from equilibrium. Comparing these two Hamiltonians gives us the idea to think of Q as p and x as Φ. As further motivation we recall that p and x satisfy the canonical equations of motion

$$\frac{\delta H}{\delta p} = \dot{x} \qquad \frac{\delta H}{\delta x} = -\dot{p} \tag{2.1.6}$$

and we see that Q and Φ also satisfy these equations identically

$$\frac{\delta H}{\delta \Phi} = \frac{\Phi}{L} = I = \dot{Q} \qquad \frac{\delta H}{\delta Q} = \frac{Q}{C} = V = -L\dot{I} = -\dot{\Phi} \tag{2.1.7}$$

	Classic Mechanical	Classic Electronic	Quantum Mechanical	Quantum Electronic
Displacement	x	Φ	$\hat{x}$	$\hat{\Phi}$
Flow	p	Q	$\hat{p} = -i\hbar\frac{d}{dx}$	$\hat{Q} = -i\hbar\frac{d}{d\Phi}$
Force Proportionality	m	C	m	C
Restoring Proportionality	k	$\frac{1}{L}$	k	$\frac{1}{L}$
Resonant Frequency	$\omega = \sqrt{\frac{k}{m}}$	$\omega = \frac{1}{\sqrt{LC}}$	$\omega = \sqrt{\frac{k}{m}}$	$\omega = \frac{1}{\sqrt{LC}}$
Commutation Relations	-	-	$[\hat{x}, \hat{p}] = i\hbar$	$\left[\hat{\Phi}, \hat{Q}\right] = i\hbar$

TABLE 2.1.1. Relationship of variables between the mechanical and electronic harmonic oscillator as well as classically and quantum mechanically.

Let us assume this relationship is true for all the variables of these systems and then we can make the jump from classical to quantum quite easily as shown in Table 2.1.1. We may now write the quantum Hamiltonian of the LC circuit as

$$H_{\mathrm{qm,LC}} = \frac{\hat{Q}^2}{2C} + \frac{\hat{\Phi}^2}{2L} = -\frac{\hbar^2}{2C}\frac{\delta^2}{\delta\Phi^2} + \frac{1}{2L}\Phi^2 \tag{2.1.8}$$

This has all the properties of the mechanical harmonic oscillator. Specifically, the energy eigenvalues and eigenvectors are characterized by an integer n such that

$$E_{\mathrm{n,LC}} = \hbar\omega\left(n + \frac{1}{2}\right)$$

with a Dirac notation of $|n\rangle$ to define the basis state of the system.

We can take this a step further and put this Hamiltonian into second quantization form. Recalling the creation and annihilation operators for the mechanical harmonic oscillator were $\hat{a}_{\mathrm{mec}} = \frac{1}{\sqrt{2m\hbar\omega}}\left(im\omega\hat{x} + \hat{p}\right)$[1], we can immediately write the corresponding operators using Table 2.1.1. It is convention to write these operators in terms of the characteristic impedance of the circuit $Z_{\mathrm{C}} = \sqrt{\frac{L}{C}}$ so the equations are

$$\begin{cases} \hat{a}_{\mathrm{LC}} = \frac{1}{\sqrt{2\hbar Z_{\mathrm{C}}}}\left(Z_{\mathrm{C}}\hat{Q} + i\hat{\Phi}\right) & \text{anhiliation} \\ \hat{a}^{\dagger}_{\mathrm{LC}} = \frac{1}{\sqrt{2\hbar Z_{\mathrm{C}}}}\left(Z_{C}\hat{Q} - i\hat{\Phi}\right) & \text{creation} \end{cases} \tag{2.1.9}$$

We can now rewrite the Hamiltonian simply as

$$H = \hbar\omega(\hat{a}^{\dagger}_{\mathrm{LC}}\hat{a}_{\mathrm{LC}} + \frac{1}{2}) \tag{2.1.10}$$

If the system is in state $|n\rangle$ then

$$a^{\dagger}|n\rangle = \sqrt{n+1}\,|n+1\rangle \qquad a|n>= \sqrt{n}\,|n-1\rangle \qquad a^{\dagger}a\,|n\rangle = n\,|n\rangle$$

and we can also recognize $a^{\dagger}a$ as the number operator $\hat{n}$. The commutation relation between these operators is exactly as that for the mechanical harmonic oscillator, $\left[a, a^{\dagger}\right] = 1$.

You may have asked yourself, what would happen if we chose the variables differently so that Q was x and p was Φ? Since these variables, Q and Φ, are canonical variables, then it should not be too surprising to realize that the analysis would have taken a slightly different path, but produced identical results. This is equivalent to the concept of analyzing a mechanical harmonic oscillator system in either the position or momentum basis. In this other analytical path Table 2.1.1 would look different, for example $m = L$ and

[1]Note that in most texts the convention is to make the momentum term the imaginary term in the factoring of the Hamiltonian to define the creation and annihilation operators, however in principle this assignment is arbitrary. For completeness with the results we have used thus far in this text, the authors have chosen to define the position component to be the imaginary term, breaking with convention.

$k = \frac{1}{C}$ etc., but if you test for yourself you will arrive at identical results. The method used in this text follows convention, but if it seems counter-intuitive to you there should be no hesitation in analyzing in this other representation. Though care should be taken to explicitly state your chosen basis.

Finally, it is also possible to have used the variables V and I to arrive at nearly the same conclusions. The above analysis would be identical with the substitutions

$$\hat{V} = \frac{\hat{Q}}{C} \qquad \hat{I} = \frac{\hat{\Phi}}{L} \tag{2.1.11}$$

2.2. Controlling Our Quantum Circuits

So what if we had not neglected a resistance R in the circuit? For simplicity in our analysis let us put a resistor in parallel with our inductor and capacitor as in Figure 2.2.1 and ignore any incoming current. Kirchoff's circuit laws tell us the net current at the junction is zero, so $I_{\mathrm{L}} = I_{\mathrm{R}} + I_{\mathrm{C}}$ and that the voltage across each element is equal. Noting that $I_R = \frac{V}{R}$, $I_C = C\frac{dV}{dt}$ and $V = -L\frac{dI_L}{dt}$ we can write a dynamic equation for the current through the inductor as

$$CL\frac{d^2}{dt}I_L + \frac{L}{R}\frac{d}{dt}I_{\mathrm{L}} + I_{\mathrm{L}} = 0 \tag{2.2.1}$$

This equation has a general solution of

$$I(t)_{\mathrm{L}} = e^{-\beta t}\left[A_1 e^{t\left(\beta^2-\omega_0^2\right)^{1/2}} + A_2 e^{-t\left(\beta^2-\omega_0^2\right)^{1/2}}\right] \tag{2.2.2}$$

where $\beta = \frac{1}{2RC}$ and $\omega_0 = \frac{1}{\sqrt{LC}}$. We can see the general solution is sinusoidal in nature with an amplitude that exponentially decays proportional to the damping constant β. The characteristic amplitude decay time for this circuit is then defined as

$$\tau_{\mathrm{amp}} = 2RC \tag{2.2.3}$$

This has the obvious consequence that if we put energy into our oscillator it will dissipate over time. This may cause problems if, for example, we attempt to set our qubit into an excited state to be used later, but we wait too long and the energy has already dissipated. A simple solution is to decrease the resistance in the circuit to give a longer decay time. Superconductors have extremely small resistance, thus one way to increase our control over the circuit is to cool it down into the superconducting regime for the component material of the circuit. (if we increase R then τ_{amp} gets bigger so something has to be wrong with what i just said)

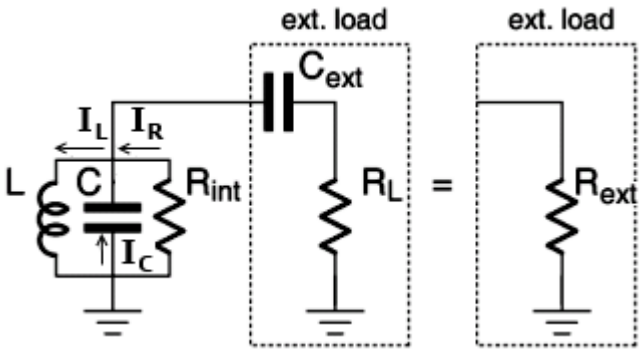

FIGURE 2.2.1. Parallel LRC circuit

Of course in order for our circuit to be useful we need to couple it to the environment so that we may change and measure the system at our convenience. This coupling adds increased parasitic effects on the harmonic oscillator including increased dissipation. In principal one may model the environment as a frequency dependent element of impedance in parallel with the LC circuit and using circuit analysis show that this has the added effect of shifting the resonant frequency of the oscillator. It will also change the net resistance and capacitance of the harmonic oscillator effectively altering the decay constant. With this analysis we would have that $C_{\sum} = C_{\mathrm{int}} + C_{\mathrm{ext}}$ and $\frac{1}{R_{\sum}} = \frac{1}{R_{\mathrm{int}}} + \frac{1}{R_{\mathrm{ext}}}$ and $\tau_{\sum} = 2C_{\sum}R_{\sum}$.

If we were to add as an input a sinusoidal driving current of frequency, ν, we could plot a spectral response of the current through the inductor and find a Lorentzian curve about the resonant frequency of the system. The equation would be

$$I_L(\nu) = (I_{\max})^2 \frac{\delta\nu}{\pi\left[(\nu-\nu_{\mathrm{r}})^2 + \delta\nu\right]} \tag{2.2.4}$$

where $\delta\nu$ is the full width half-maximum of the curve and ν_r is the resonant frequency. We could also define a quality factor Q as

$$Q = \frac{\nu_r}{\delta\nu} = \frac{\text{input power}}{\text{dissipated power}} \tag{2.2.5}$$

The full width half maximum, $\delta\nu$ is related to the dissipation in the system and thus correlated with the quality factor. Ideally, for measurement and control of the system we need high quality factors. This again shows that we need minimal resistance in the circuit for practical use.

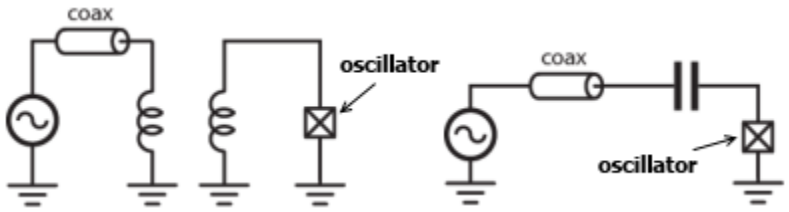

FIGURE 2.2.2. Two simple coupling schemes using inductors and capacitors

There are various engineering schemes for decoupling the harmonic oscillating circuit from the environment, the two most simplistic schemes involve physically separating the oscillator circuit and the external circuit via either a capacitor or an inductor. There is a catch 22, however, when designing the decoupling because the coupling itself is also the mechanism for control of the oscillator. Obviously, if you completely decouple the circuits by perhaps making the coupling capacitor separation infinite, than you no longer have any control of the system. Thus, some happy middle ground must be used.

Another important aspect of controlling our system for quantum computation is knowledge and control of the state of the system. The computational basis of a qubit is two levels and we need absolute control over which level the system is in. Using either Fermi-Dirac, Bose-Einstein or Maxwell-Boltzmann distribution functions, depending on the nature of the system, we know the probability of a certain energy level being occupied is dependent on temperature. In the limit $T \to 0$ the probability the system is in the ground state approaches unity. In general we need to make sure that the energy gap between the ground state and the first excited state is much larger than the thermal energy of the system. This will ensure that the system does not enter the first excited state without our deliberate desire.

The energy spectrum of super-conductors is in many ways ideal for these considerations. When a metal is at room temperature the energy spectrum for the valence electrons is a continuum. However, as it cools and reaches a critical temperature, these electrons begin to bind together into Cooper-pairs. The bound state is between two opposite spin electrons with a typical binding energy, Δs, on the order of a meV. The pair form a Bosonic state with a spin and angular momentum of zero. The charge is of course $2e$. The colder the metal gets the more binding occurs until nearly all of the electrons have formed cooper-pairs. Since they

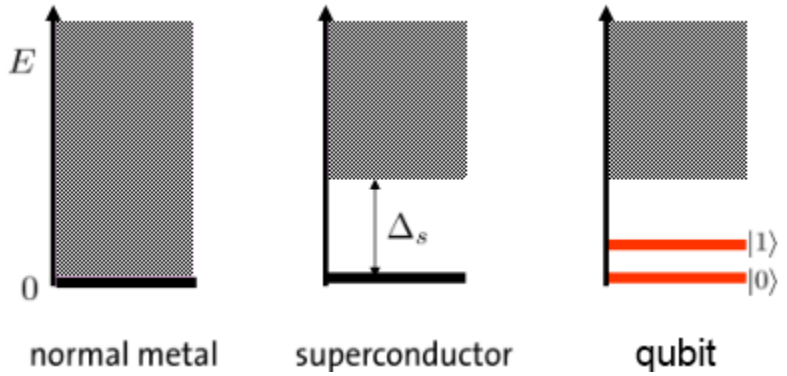

FIGURE 2.2.3. Energy spectra of metal room temperature, at superconducting temperature and engineered to have a split in the ground state energy level.

are bosons they can all simultaneously occupy the same state and at sufficiently low temperature they will all reach the ground state. Through clever engineering one can in principle design a system which will split this energy level, into two energy levels and we will then have our qubit. This process would be akin to hyperfine splitting of energy states in an atom when it is in the presence of an external magnetic field. This is depicted in Figure 2.2.3.

It should be noted that the analysis of this section has been purely classical and one might wonder if such an analysis is applicable to a quantum system. Indeed this analysis is not complete, however, qualitatively and in many respects quantitatively this analysis is accurate. If the reader is interested in a more complete and quantum description of dissipation in harmonic oscillators this can often be found in quantum optics textbooks. The topic is closely related to the master equations and non-unitary Hamiltonian analysis.

In conclusion, our need to control the harmonic oscillator's dissipation time, its energy state, as well as the need for a computational basis, has lead us to the use of superconducting circuits. As a final note, typical temperatures for actual quantum circuits are on the order of $10^{-2}\,\mathrm{K}$ with quality factors on the order of 10^4. This is in large part due to the limitation on the size of inductors and capacitors which, practically speaking get only as small as $1\,\mathrm{nH}$ and $1\,\mathrm{pF}$ respectively. This leads to a typical resonant frequency on the order of 5 GHz.

2.3. Linear vs. Nonlinear Oscillators (Josephson Junction)

FIGURE 2.3.1. a)Harmonic energy spectrum b)An-harmonic energy spectrum

Given that we now know the superconducting LC circuit will have discrete energy levels as $E_{\mathrm{n,LC}} = \hbar\omega\left(n+\frac{1}{2}\right)$, we could use this to construct a qubit basis using any two levels of the system. We could also in principle create superposition states in the magnetic flux or the charge basis. However, in practice there is one glaring problem when we look at the energy spectrum. Specifically, all of the energy levels are separated by an identical amount of energy. When attempting to induce a transition from the ground state to the first excited state, we may actually induce a transition from the first excited state to the second, or a transition from any two states in the system. This will be a problem for any linear oscillator. Ideally we need a circuit element to be nonlinear to introduce some an-harmony to the energy spectrum.

One solution to this problem has been the Josephson Junction, named after the British physicist who first derived the theoretical ground work for such a junction. The junction itself is nothing more than two superconducting materials separated by a small insulator as depicted in Figure 2.3.2. What Josephson discovered is that the Cooper-pairs discussed in the previous section, will tunnel through the insulating barrier and cause some unique effects. The most useful aspect is that it will also act like a non-linear inducting element.

Josephson derived the following properties of such a junction. First, the current through the junction will be

$$I_{\mathrm{J}} = I_{\mathrm{C}}\sin\delta = I_{\mathrm{C}}\sin\left(\frac{2\pi\Phi(t)}{\Phi_0}\right) \tag{2.3.1}$$

where I_{C} is called the critical current and it is a phenomenological property of the junction.

$$\delta = \delta_2 - \delta_1 = \frac{2\pi\Phi(t)}{\Phi_0} \tag{2.3.2}$$

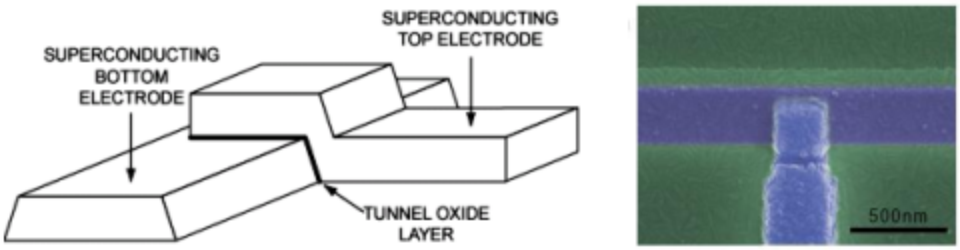

FIGURE 2.3.2. A Josephson Junction

is the difference in the phase angles of the quantum state of the systems on either side of the junction. $\Phi(t)$ is the magnetic flux through the junction, while Φ_0 is the Flux quantum which has a value of

$$\Phi_0 = \frac{h}{2e} \tag{2.3.3}$$

and is the quantization unit of a magnetic flux field.

He also derived the voltage across the junction as

$$V_J = \frac{\Phi_0}{2\pi}\frac{d\delta}{dt} = \frac{d\Phi}{dt} \tag{2.3.4}$$

Now using equation 2.3.1 we find that

$$\frac{dI}{dt} = I_{\mathrm{C}}\cos\delta\frac{d\delta}{dt} \rightarrow \frac{d\delta}{dt} = \frac{dI}{dt}\frac{1}{I_{\mathrm{C}}\cos\delta} \tag{2.3.5}$$

so that

$$V_J = \frac{\Phi_0}{2\pi I_{\mathrm{C}}\cos\delta}\frac{dI}{dt} \tag{2.3.6}$$

which looks like an induction equation $V = -L\frac{dI}{dt}$. This derives for us the so called Josephson inductance of the junction

$$L_{\mathrm{J}} = \frac{\Phi_0}{2\pi I_{\mathrm{C}}}\frac{1}{\cos\delta} = L_{\mathrm{J}_0}\frac{1}{\cos\delta} \tag{2.3.7}$$

We can see that this inductance is nonlinear. Exactly what we were looking for.

The energy of this non-linear inductor is

$$E_{\mathrm{J}} = \int VI\,dt = \frac{I_{\mathrm{C}}\Phi_0}{2\pi}\cos\delta = E_{\mathrm{J}_0}\cos\delta \tag{2.3.8}$$

A final important property of the Josephson Junction is that it is non-dissipative, which means it has no internal resistance. This makes it an ideal candidate as an element in a superconducting quantum circuit.

Figure 2.3.3 shows three different styles of depicting the Josephson Junction in a circuit. It is important to note that the Josephson Junction also has an internal capacitance which can be considered to be in parallel with the tunneling/inductive part.

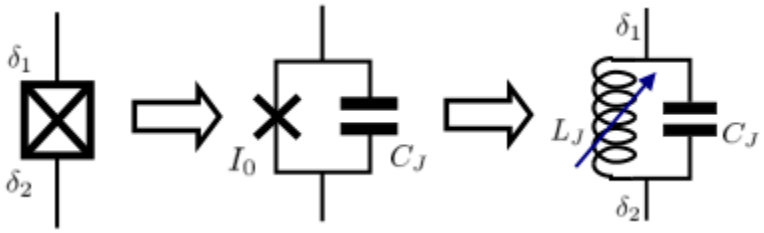

FIGURE 2.3.3. Common ways of depicting a Josephson Junction in a circuit diagrams.

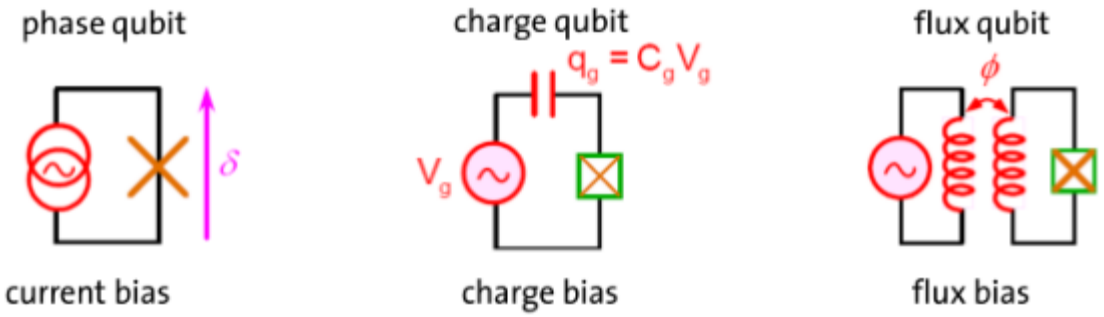

FIGURE 2.4.1. Three Different types of qubits which use Josephson Junctions

2.4. The Cooper-Pair Box Charge Qubit

When trying to construct a functioning quantum mechanical electronic circuit for quantum information processing we started with our classical understanding of a parallel RLC circuits. We were inspired by the the analogy between the electronic and mechanical harmonic oscillators to derive the quantum Hamiltonian for an LC circuit. Upon deriving the energy levels for such a system we realized a problem will occur controlling the transitions between two states because the energy levels are all separated by an identical amounts of energy. We then learned about Josephson Junctions as a solution to this problem because they act like a non-linear inductor. Now we need to see how this new element alters the Hamiltonian and solve for the new energy levels of this system.

There are a variety of ways we could construct the circuit which will have varying paths of analysis and usage. The three common setups either use a coax line, a capacitor or an inductor to couple an external voltage to the Josephson Junction as depicted in Figure 2.4.1. The coax-line creates a natural phase basis for a qubit, a capacitor forms a natural charge basis, and the inductor forms a natural flux basis. Each way has its merits and demerits, but for the purposes of this course and due to its current popularity we will focus on the capacitor setup which is called a Cooper-Pair Box.

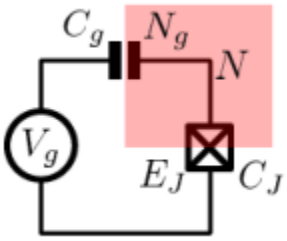

FIGURE 2.4.2. A Cooper-Pair Box

Figure 2.4.2 shows a simple Josephson Junction connected to an external voltage source through a gate capacitor. Our analysis will begin conceptually from the point of view of the "island" also depicted in the figure. This island is isolated from the outside world via the capacitors dielectric material and the Josephson Junction insulating gap. Initially, when there is no gate voltage, the island is charge neutral. When the gate voltage is turned on the charges will begin to polarize as we would expect. We can imagine surface charges being induced on the island to try and cancel the external potential, internally. However, these net charges are only a result of the already present charges on the island rearranging themselves according to the externally applied force from the gate voltage. No new charges have been introduced to the island. There is however, a bridge onto the island across the Josephson Junction. As the island polarization increases, Cooper-pairs will being tunneling across the junction to try to re-neutralize the polarization. This causes an actual increase in the number of charges on the island. If we continue to increase the gate voltage, Cooper-pairs will continue to tunnel onto the island. If we remove the voltage, these extra Cooper-pair charges will tunnel back off of the island returning the system to its original state.

From this conception we can envision a qubit as the presence or absence of extra Cooper-pairs on the island from the original number. In the most simplistic case, the ground state would be no extra Cooper-pairs on the island, while the first excited state is exactly one extra Cooper-pair on the island. A superposition state would occur when there is some non-unit probability, α, of a single Cooper-pair tunneling through the Josephson Junction. Now that we have an idea of what we might be looking for, we can play with the Hamiltonian to try and derive these results quantitatively.

The Hamiltonian is as it was before a sum of the total energy being stored in the electric and magnetic fields in the circuit elements.

$$H_{\mathrm{JC_g}} = H_{\mathrm{el}} + H_{\mathrm{mag}} \tag{2.4.1}$$

There are electric fields being stored in the capacitors of the system so that $H_{\mathrm{el}} = \frac{\hat{Q}_{\sum}^2}{2C_{\sum}}$, which is identical to before except now we have more than one capacitor as well as extra Cooper-pair charges to account for. Our envisioned basis and the relevant dynamics of our circuit are related to the extra number of Cooper-pair charges on the island. Therefore the total charge we are concerned with is the difference in Cooper-pair charges, which have tunneled onto the island, and the effective number of charges which have built up on the gate capacitor. Quantitatively $Q_{\sum} = Q_{\mathrm{CP}} - Q_{\mathrm{G}}$.

$C_{\sum}$ is the net capacitance of the island and in this case would be $C_{\sum} = C_{\mathrm{G}} + C_{\mathrm{J}} + C_{\mathrm{ext}}$. From the point of view of the island the gate capacitor and the junction capacitor are in parallel so their net capacitance is additive and we have added an extra term C_{ext} to represent unforeseen external capacitance between this island and the environment.

Since we were looking for a basis in terms of Cooper-pair occupation on the island, we should change from a generic charge $\hat{Q}$ to a number representation basis $\hat{N}_{\mathrm{CP}}$ of Cooper-pairs. The number of cooper-pairs on the island is discrete and is $2e\hat{N}_{\mathrm{CP}} = \hat{Q}_{\mathrm{CP}}$. Remember a Cooper-pair has a net charge of $2e$ since it is a pair of electrons. We can *normalize* the capacitor charge as also being some number of Cooper-pair charges such that $Q_{\mathrm{G}} = 2eN_{\mathrm{G}} = C_{\mathrm{G}}V_{\mathrm{G}}$ and we note that this number of charges is continuous compared to the Cooper-pair particle number. That is to say that V_G can in principle be adjusted along a continuous spectrum from $-\infty$ to ∞. We can therefore write

$$H_{\mathrm{el}} = \frac{4e^2}{2C_{\sum}}\left(\hat{N}_{\mathrm{CP}} - N_{\mathrm{G}}\right)^2 \tag{2.4.2}$$

The constant term in front is called the charging energy

$$E_{\mathrm{C}} = \frac{4e^2}{2C_{\sum}} \tag{2.4.3}$$

.

The qualitative and quantitative analysis used up to this point has been classical, and again the reader should be cautioned that we have not fully pictured nor properly derived these results. However, the resulting Hamiltonian is in fact the correct Hamiltonian which would be derived from stricter quantum considerations. Of course, however, we have not considered dissipation or other forms of interaction dynamics. We will consider these in some detail later. Our intention at this point is to understand the principle characteristics and dynamics of this new system.

This purely electrical Hamiltonian is graphed in Figure 2.4.3. As we can see this part of the Hamiltonian is proportional to N_{G}^2 and is therefore parabolic in nature. However, there will be a parabola centered at every discrete value of N_{CP}. This creates a band like structure of the energy levels which are depicted with different colors in the figure. As a side note, this spectrum is identical to the free electron spectrum in a one dimensional lattice.

This is of course only half the picture since we have yet to account for the magnetic part of the Hamiltonian. As we found before, the Josephson Junction acts like an inductor and will be storing energy in its magnetic field. The energy in the junction will be

$$H_{\mathrm{mag}} = -E_{\mathrm{J}_0}\cos\hat{\delta} \tag{2.4.4}$$

so the final Hamiltonian becomes

$$H_{\mathrm{JC_G}} = E_{\mathrm{C}}\left(\hat{N}_{\mathrm{CP}} - N_{\mathrm{G}}\right)^2 - E_{\mathrm{J}_0}\cos\hat{\delta} \tag{2.4.5}$$

It would be ideal to put this equation in terms of one of the operators and use that operator as a basis state. Since $\hat{N}_{\mathrm{CP}} = \frac{\hat{Q}}{2e}$ and $\hat{\delta} = 4\pi e h\hat{\Phi}$ while $\left[\hat{\Phi},\, \hat{Q}\right] = i\hbar$ we find upon substitution that $\left[\hat{\delta}, \hat{N}_{\mathrm{CP}}\right] = i$ and therefore, to no surprise, these are conjugate variables. We expect the number operator $\hat{N}_{\mathrm{CP}}$to return the number of Cooper-pairs on the island in a particular state, using Dirac notation we would have $\hat{N}_{\mathrm{CP}}\left|N\right\rangle =$

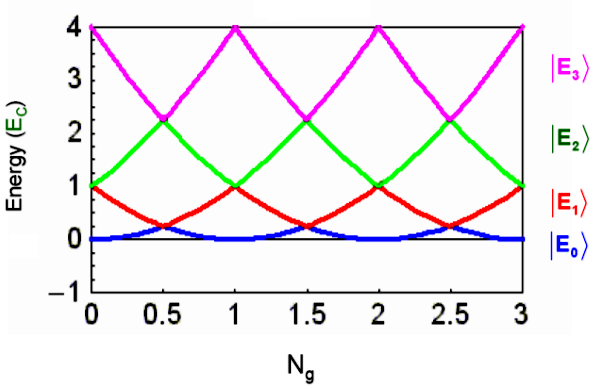

FIGURE 2.4.3. The electric part of the Hamiltonian, H_{el}, for a Cooper-pair Box

$n_{\text{CP}} |N\rangle$. As expected these states satisfy the relations

$$\hat{N} |N\rangle = n |N\rangle$$
$$\sum_N |N\rangle \langle N| = \mathcal{I}$$
$$\langle M \mid N\rangle = \delta_{mn}$$

where $\mathcal{I}$ is the identity. In this way we could use either of these variables as a convenient notation for the basis states.

Being conjugate variables we can transform between the charge number basis and the phase basis by

$$|\delta\rangle = \frac{1}{\sqrt{2\pi}} \sum_N e^{iN\delta} |N\rangle \tag{2.4.6}$$

and we find that

$$e^{\pm i\delta} |N\rangle = |N \pm 1\rangle \tag{2.4.7}$$

We can rewrite equation 2.4.4 using the Euler relation as $H_{mag} = -\frac{E_{\text{J}_0}}{2}\left(e^{i\delta} + e^{-i\delta}\right)$ in order to use 2.4.7 and finally write the Hamiltonian completely in the number basis as

$$\hat{H}_{\text{JC}_\text{G}\text{N}_\text{basis}} = \sum_N \left[E_\text{C} \left(\hat{N}_\text{CP} - N_\text{G}\right)^2 |N\rangle \langle N| - \frac{E_{\text{J}_0}}{2} \left(|N\rangle \langle N+1| + |N+1\rangle \langle N|\right)\right] \tag{2.4.8}$$

Of course if we wanted we could instead write this in the phase basis as

$$\hat{H}_{\text{JC}_\text{G}\delta_\text{basis}} = E_\text{C} \left(-i\frac{d}{d\delta} - N_\text{G}\right)^2 - E_{\text{J}_0} \cos\hat{\delta} \tag{2.4.9}$$

Now that we have a final Hamiltonian, it is a mathematical activity to find the Eigenvalues and Eigenvectors of the system. However, this is not very instructive for our concerns. What is constructive is concerning ourselves with a two-level approximation since this will show the relevant characteristics for our qubit. In this limit our Hamiltonian becomes

$$\hat{H}_{\text{JC}_\text{G}\text{N}_\text{basis}} = E_C N_G^2 |0\rangle \langle 0| + E_C \left(1 - N_G\right)^2 |1\rangle \langle 1| - \frac{E_{\text{J}_0}}{2} \left(|0\rangle \langle 1| + |1\rangle \langle 0| + |1\rangle \langle 0| + |0\rangle \langle 1|\right)$$

the result can be put in terms of the Pauli-spin matrices,

$$\hat{H}_{\text{JC}_\text{G}\text{N}_\text{basis}} = -\frac{E_\text{C}}{2} \left(1 - 2N_\text{G}\right) \hat{\sigma}_z - \frac{E_{\text{J}_0}}{2} \hat{\sigma}_x \tag{2.4.10}$$

From the secular equation we can solve for the energy eigenvalues and find

$$E_\pm = \pm\frac{1}{2}\sqrt{E_C^2 + E_{\text{J}_0}^2 + 4N_G E_C^2 \left(N_G - 1\right)} \tag{2.4.11}$$

This distribution is plotted in Figure 2.4.4a and it should be quite clear that the magnetic term of the Hamiltonian, which is proportional to the Josephson energy, effectively creates energy gaps at the degeneracy points. In Figure 2.4.4b we see the gap size between the ground state and the first excited stated is approximately the Josephson Energy. However, the gap size decreases between increasing energy levels. This is exactly what we wanted since this will help us control transitions assuming we can also get $E_{J_0} \gg k_B T$. We have effectively created a tunable atom!

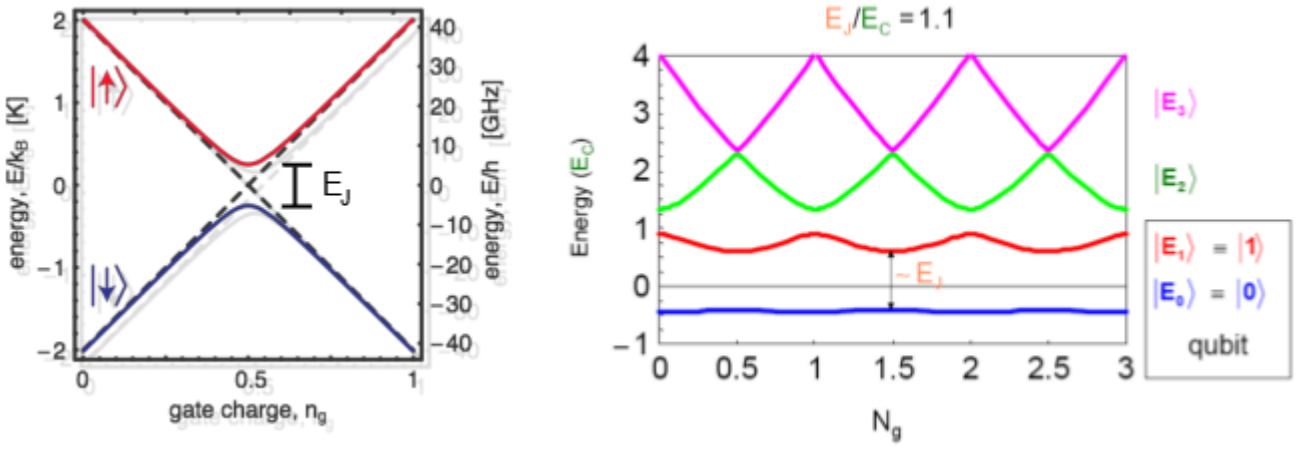

(A) (B)

FIGURE 2.4.4. Energy eigenstates of a Cooper-Pair Box in (A) the two-level approximation and (B) the general case.

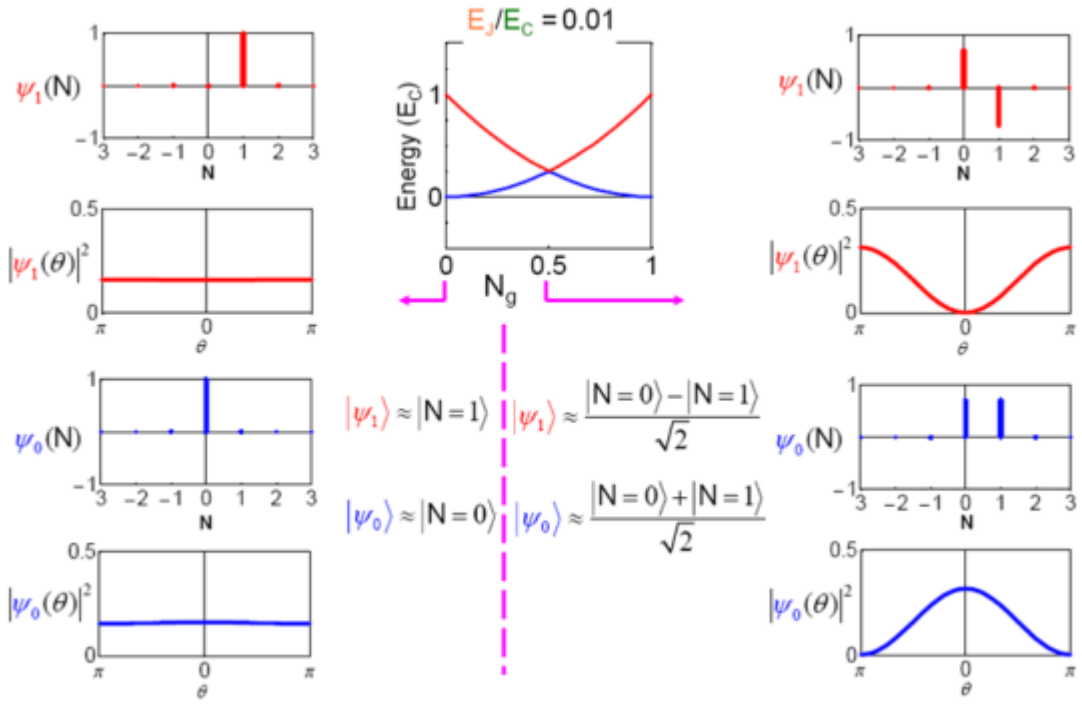

FIGURE 2.4.5. Energy spectrum and wave functions for a Cooper-Pair Box with $E_{J_0} \ll E_C$. The left side graphs correspond to the case $N_g = 0$, while the right side are for $N_g = 0.5$.

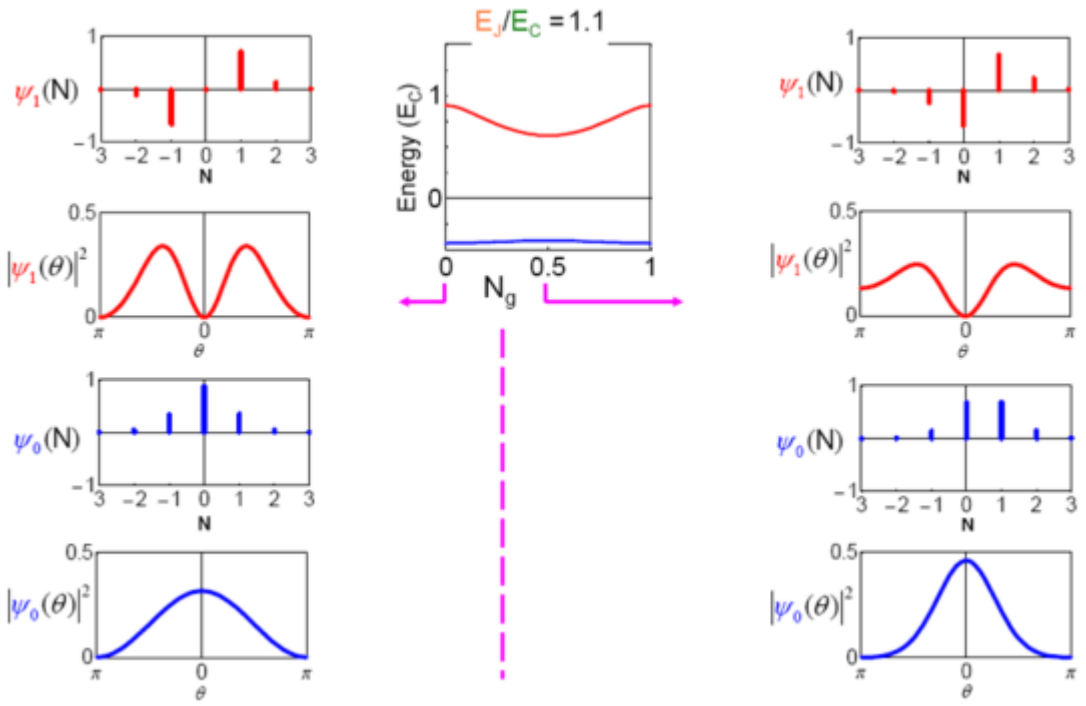

FIGURE 2.4.6. Energy spectrum and wave functions for a Cooper-Pair Box with $E_{J_0} \ll E_C$. The left side graphs correspond to the case $N_g = 0$, while the right side are for $N_g = 0.5$.

For a deeper understanding we plot the wave function and the square of the wave function in the number and phase basis as well as the energy levels for the two cases $E_{J_0} \ll E_C$ and $E_{J_0} \cong E_C$.

Figure 2.4.5 shows the case for $E_{J_0} \ll E_C$. For $N_G = 0$ we see the wave function in the number basis are in coherent states, either $|0\rangle$ or $|1\rangle$. However if $N_G = 0.5$ we find that the system is in an entangled state either symmetrically or anti-symmetrically depending on the energy level of the system. One can also see the conjugate pair relationship between the number basis and the phase basis by noting that a near perfect coherent state in the number basis corresponds to a completely flat and unknown phase basis state.

Figure 2.4.6 is the case for $E_{J_0} \cong E_C$. We see the picture becomes a bit more complicated now as there are no definite coherent states. Even when $N_G = 0$ the wave function is a linear combination of the system with various amounts of Cooper-Pairs on the island. Though, the amplitudes do fall off quickly.

Finally, the energy levels in the limit $E_{J_0} \gg E_C$ are plotted in Figure 2.4.7. As it turns out, this case is the most ideal for the lab. This is due to the extremely flat nature of the bottom two energy levels which creates a system highly resilient to noise. The graphs which we have plotted in this text are the idealized, theoretical case which do not take into account a lot of real world terms such as noise, de-phasing, measurement uncertainty, and dissipation. In the lab trying to reproduce these energy level graphs would result in fluctuations of the general shape and at points near the energy gap, for example in Figure 2.4.5, it would be nearly impossible to tell which level the system is in. When the levels are flat it becomes much more difficult for these fluctuations to cause overlap and therefore one can with greater certainty determine the level of the system. This is just a quick example of one feature which make the large Josephson energy limit ideal, there are however others which we will not discuss here.

2.5. Tuning the Junction

Though it has already been implicitly stated that we can tune this qubit to nearly our exact specifications within the limits of current technology, it will not be a waste to reemphasize this capability. Again looking at the Hamiltonian and the eigenenergies of the two level system, we recognize the relevant parameters are the charging energy E_C, the number of gate charges N_G and the Josephson Energy E_J.

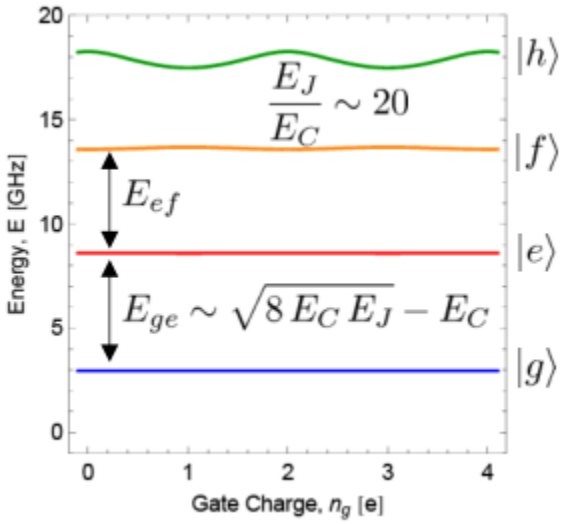

FIGURE 2.4.7. Energy spectrum for a Cooper-Pair Box with $E_{J_0} \gg E_C$

The first two terms are relatively easy to control. The charging energy in equation 2.4.3 is inversely proportional to the net capacitance on the island E_C. Our desired regime for the qubit was in the limit $E_{J_0} \gg E_C$ which can be obtained by decreasing the value of E_C. Without influencing the relative dynamics of our qubit, we may simply add more capacitors in parallel with Josephson Junction, thereby increasing the net capacitance of the island. The gate charge N_G is directly proportional to the externally applied voltage, which of course we control.

The Josephson energy, however, is a bit more difficult to understand our control over. The term itself is proportional to a constant dependent on the critical current, and the cosine of the phase difference across the junction. The critical current is directly proportional to the ease at which Coop-pairs can tunnel through the junction. Therefore, this value can be controlled in fabrication by the surface area and the thickness of the tunnel. The larger the surface area, and the thinner the insulting layer, the larger the critical current can be. These parameters are tunable to our specifications within the limit of fabrication techniques. However, once the junction is set, they can not be adjusted.

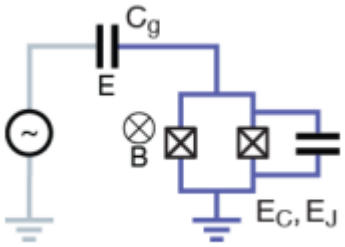

FIGURE 2.5.1. Transmon circuit diagram

The phase difference is dependent on the magnetic flux through the junction which is in principle a real time quantity we could adjust by applying an external magnetic field. Unfortunately, the necessary magnetic fields required to have an effect on a single junction are much larger than is practical. However, clever engineering can alleviate this problem. Without formal proof, we state that two Josephson Junctions in parallel effectively change the dependence of the cosine term in the Josephson energy from the magnetic flux through the individual junction, to the magnetic flux of the loop of the junctions. Since the loop has a much larger area than the individual junctions, the necessary magnetic field is much smaller to control the cosine parameter. We call this type of circuit a Transmon and it is depicted in Figure 2.5.1.The Transmon Hamiltonian is

$$H_{\text{transmon}} = \frac{E_C}{2}(\hat{N}_{CP} - N_G)^2 - E_{J_0}\cos\underbrace{\left(\pi\frac{\Phi_{\text{ext}}}{\Phi_0}\right)} \tag{2.5.1}$$

where Φ_{ext} is the magnetic flux through the loop of Josephson Junctions. These Transmons easily reproduce the conditions for our desired circuit where $E_{J_0} \gg E_C$.

2.6. Manipulating the Qubit

At the end of the day, we want to use this qubit for quantum computation so controlling the qubit state is extremely important. Our control should be able to take our qubit and transform it from any state to any other state on the Bloch sphere. Qualitatively from our knowledge of classical oscillators we expect to be able to control the state of the qubit by applying a sinusoidal driving force. If the frequency of the driving force is near the transition frequency of the oscillator, and the oscillator is in the ground state initially, we expect the oscillator to transition from the ground state to an excited state. Our goal now is to see exactly how the driving force will affect the qubit.

By coupling a driving voltage to the gate capacitor we can write N_{G} in equation 2.4.10 as a sum of a static component and a time dependent component. Such that $N_{\mathrm{G}} = N_{\mathrm{G}}^0 + N_{\mathrm{G}}(t)$ and for simplicity we will set $N_{\mathrm{G}}^0 = \frac{1}{2}$ and $N_{\mathrm{G}}(t) = A\cos(\omega_d t + \phi)$. This makes our Hamiltonian

$$H_{qb} = E_C A \cos\left(\omega_d + \phi\right)\hat{\sigma}_z - \frac{E_{\mathrm{J}}}{2}\hat{\sigma}_x \tag{2.6.1}$$

performing a change of basis by rotating our frame by $\pi/2$ about the y-axis we get $\hat{\sigma}_z \to \hat{\sigma}_x$ while $\hat{\sigma}_x \to -\hat{\sigma}_z$ giving us

$$H'_{qb} = \bar{A}\cos(\omega_d t + \phi)\hat{\sigma}_x + \frac{E_{\mathrm{J}}}{2}\hat{\sigma}_z \tag{2.6.2}$$

In matrix form $\hat{\sigma}_x = \begin{bmatrix} 0 & 1 \\ 1 & 0 \end{bmatrix}$ which corresponds exactly to the sum of the raising and lowering operators of a two level system. Defining $\sigma^{\pm}$ such that $\hat{\sigma}^+ |g\rangle = |e\rangle$ and $\hat{\sigma}^- |e\rangle = |g\rangle$ we find from $\hat{\sigma}^{\pm}_{ij} = \langle i| \sigma^{\pm} |j\rangle$ that $\hat{\sigma}^+ = \begin{bmatrix} 0 & 0 \\ 1 & 0 \end{bmatrix}$ while $\hat{\sigma}^- = \begin{bmatrix} 0 & 1 \\ 0 & 0 \end{bmatrix}$ and therefore $\hat{\sigma}_x = \hat{\sigma}^+ + \hat{\sigma}^-$.

Our next step is to go into a rotating frame, which rotates at the frequency of the driver. This will allow us to see how the qubit is changed relative to the applied field, as apposed to the lab frame where both would change during the interaction. Since we do not care about the state of the field, but only the qubit itself, our rotating frame should be advantageous. To change to a rotating frame we use the unitary transformation

$$U_{rot} = \exp[i\frac{\omega}{2}\hat{\sigma}_z] \tag{2.6.3}$$

The Schrodinger equation transforms like

$$U_{rot} H |\psi\rangle = U_{rot} i\hbar \frac{d}{dt} |\psi\rangle \tag{2.6.4}$$

but we need to change the basis as well so that

$$U_{rot} |\psi\rangle = |\omega\rangle \tag{2.6.5}$$

so changing the basis too gives us

$$\begin{aligned} U_{rot} H U_{rot}^\dagger U_{rot} |\psi\rangle &= U_{rot} i\hbar \frac{d}{dt}\left(U_{rot}^\dagger U_{rot} |\psi\rangle\right) \\ U_{rot} H U_{rot}^\dagger |\omega\rangle &= U_{rot} i\hbar \left(\frac{d}{dt} U_{rot}^\dagger\right)|\omega\rangle + U_{rot} i\hbar U_{rot}^\dagger \frac{d}{dt}\left(|\omega\rangle\right) \\ \left[U_{rot} H U_{rot}^\dagger - i\hbar U_{rot}\frac{d}{dt}\left(U_{rot}^\dagger\right)\right]|\omega\rangle &= i\hbar \frac{d}{dt}\left(|\omega\rangle\right) \\ H_{rot} |\omega\rangle &= i\hbar \frac{d}{dt}\left(|\omega\rangle\right) \end{aligned} \tag{2.6.6}$$

In order to calculate H_{rot} we see how the Pauli matrices transform into this frame

$$\begin{aligned} U_{rot}\hat{\sigma}_z U_{rot}^\dagger &= \hat{\sigma}_z \\ U_{rot}\hat{\sigma}_x U_{rot}^\dagger &= \cos(\omega t)\hat{\sigma}_x - \sin(\omega t)\hat{\sigma}_y \\ U_{rot}\hat{\sigma}_y U_{rot}^\dagger &= \sin(\omega t)\hat{\sigma}_x + \cos(\omega t)\hat{\sigma}_y \\ U_{rot}\frac{d}{dt}\left(U_{rot}^\dagger\right) &= -i\frac{\omega}{2}\hat{\sigma}_z \end{aligned} \tag{2.6.7}$$

Finally, we need some mathematical trickery to make the solution look nice by splitting $\bar{A}\cos(\omega_d t+\phi)\hat{\sigma}_x$ into $\frac{\bar{A}}{2}\cos(\omega_d t+\phi)\hat{\sigma}_x - \frac{\bar{A}}{2}\sin(\omega_d t+\phi)\hat{\sigma}_x + \frac{\bar{A}}{2}\cos(\omega_d t+\phi)\hat{\sigma}_x + \frac{\bar{A}}{2}\sin(\omega_d t+\phi)\hat{\sigma}_x$. Now when we substitute in the transformed Pauli matrices the expanded terms simplify to $\cos\left[(\omega \mp \omega_d)+\phi\right]\hat{\sigma}_x \pm \sin\left[(\omega \mp \omega_d)+\phi\right]\hat{\sigma}_y$. If we go into a frame rotating at the drive frequency, $\omega = \omega_d$, then we get a constant term and a term rotating in time at twice the speed of the driving frequency. Typically, we ignore these high frequency terms since they change too quickly compared to the evolution of the system. This is called a rotating wave approximation and we shall use it again in the next section.

With all of this completed we arrive at a final Hamiltonian of the qubit being driven by a sinusoidal force in the rotating frame as

$$H_{rot} = \frac{\omega_q - \omega_d}{2}\hat{\sigma}_z + \frac{\bar{A}}{2}\left[\cos\phi\hat{\sigma}_x + \sin\phi\hat{\sigma}_y\right] \tag{2.6.8}$$

Thus the frequency of the drive causes rotations about the z-axis while the phase of the driving voltage causes rotations about the x and y axis. In this way we have complete control of the state of the qubit.

2.7. Coupling a Qubit and a Simple Harmonic Resonator

Our next step will be coupling our Cooper-Pair Box(Transmon) to a simple harmonic oscillating circuit like that in the first section of this chapter. The motivation for doing this comes from Cavity Quantum Electrodynamics. Specifically, we have recognized our Cooper-Pair Box is much like an artificial atom, which we will want to manipulate in various ways and take measurements of. In Cavity QED light interacts weakly with atoms, but amplification of this interaction can be achieved by trapping the light inside a cavity. In this way, greater control and readout of the state of the atom is possible. As we shall see in a moment by coupling our Qubit to a Linear Harmonic Resonator we will be able to create a system identical to that of a Cavity QED, which is the field of circuit QED. We will not go into the full detail, but doing this has great advantages including, increased qubit lifetime, increased control of qubit-qubit coupling through a resonator and Quantum Non-Demolition (QND) readout capabilities of the qubits.

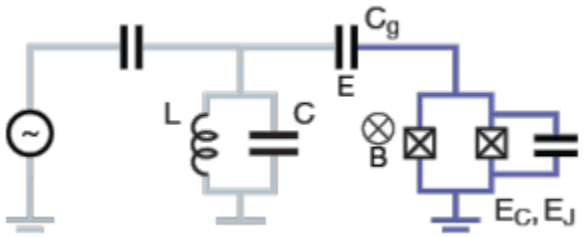

FIGURE 2.7.1. A Transmon Qubit coupled with a LC resonator

Figure 2.7.1 has a simple schematic of our system and the Hamiltonian will be the sum of the Hamiltonian of the LC resonator and the Qubit such that

$$H_{\mathrm{CQED}} = H_{\mathrm{SHO}} + H_{\mathrm{QB}} = \hbar\omega_r\left(a^\dagger a + \frac{1}{2}\right) + \frac{E_{\mathrm{C}}}{2}\left(1 - 2N_{\mathrm{G}}\right)\hat{\sigma}_z - \frac{E_{\mathrm{J_0}}}{2}\hat{\sigma}_x \tag{2.7.1}$$

Note that we have used the second quantization form of the Hamiltonian for the simple harmonic resonator and the two level Hamiltonian of the Cooper-Pair Box for the qubit.

Analyzing this equation we recognize the first term as the energy of the LC circuit resonator and it is identical to the energy of a quantized field of electromagnetic radiation trapped in a resonator cavity. Closer inspection of the third term yields that this is related to the energy level separation of our qubit, which will act as our artificial atom. The second term is related to the charging energy and thus the coupling capacitor between the two systems. This is therefore an interaction energy between our resonator and our artificial atom. We could thus look at our Hamiltonian as the sum of these three energies

$$H_{\mathrm{QED}} = H_{\mathrm{resonator}} + H_{\mathrm{interaction}} + H_{\mathrm{atom}} \tag{2.7.2}$$

If you have taken a Quantum Electrodynamics course, or studied any part of quantum optics or ion traps, this general Hamiltonian should look familiar. These QED interactions between atoms trapped in a resonator cavity have been studied for a significantly longer period than our quantum circuits and are, relatively speaking, well understood. A simple model in QED is governed by the Jaynes-Cummings Hamiltonian given by

$$H_{JC} = \hbar\omega_c\left(\hat{a}^\dagger\hat{a} + \frac{1}{2}\right) + \frac{\hbar\omega_a}{2}\hat{\sigma}_z + \frac{\hbar g}{2}\left(\hat{a}\hat{\sigma}^+ + \hat{a}^\dagger\hat{\sigma}^-\right) \tag{2.7.3}$$

ω_c is the frequency of the mode of oscillation of the radiation in the cavity and ω_a the transition frequency of the atom trapped in the cavity. g is a coupling factor and $\sigma^{\pm}$ are the raising and lower operators of the atom such that $\sigma^+ |g\rangle = |e\rangle$, while $\sigma^- |e\rangle = |g\rangle$, where $|g\rangle$ and $|e\rangle$ are the ground state and first excited state respectively. It is not necessary that you know any of this already, the main purpose of pointing it out here is as a motivation for transforming 2.7.1 into a form like 2.7.3.

As a first step to transform our given Hamiltonian into a Jaynes-Cummings form, we can see a $\pi/2$ rotation about the y-axis, i.e. a change of basis, will transform $\hat{\sigma}_z \to \hat{\sigma}_x$ and $\hat{\sigma}_x \to -\hat{\sigma}_z$ in our equation. This will put the Hamiltonians in the same basis. Now, all we have to do is manipulate the interaction part of the Hamiltonian. N_{G}, which recall is the number of charges built up on the gate capacitor, will have quantum fluctuations associated with it. In typical circuits these fluctuations are small and play no major role in the physics of the system, however in our superconducting quantum circuits these fluctuations can not be ignored. We will therefore split N_G into a classical and quantum component such that $N_{\mathrm{G}} = N_G^{CL} + N_G^{QM}$, we can set the classical component, which we control via our voltage regulator, to $1/2$ so that we can cancel the constant term. We are left with $E_C N_G^{QM} \hat{\sigma}_x$. This N_G term is related to the voltage in the resonator circuit via $N_G^{QM} = \frac{C_G}{2e}\hat{V}$ where we note that this variable is no longer continuous but discrete. Using equations 2.1.9 and 2.1.11 we can write $\hat{V} = \sqrt{\frac{\hbar\omega_r}{2C}}\left(\hat{a}^\dagger + \hat{a}\right)$. Upon substitution the interaction part becomes

$$H_{int} = E_C \frac{C_G}{2e}\sqrt{\frac{\hbar\omega_r}{2C}}\left(a^\dagger + a\right)\hat{\sigma}_x \tag{2.7.4}$$

By finding the matrix form of $\hat{\sigma}^{\pm}$ and $\hat{\sigma}_x$ we find that $\hat{\sigma}_x = \hat{\sigma}^+ + \hat{\sigma}^-$. Finally, $\left(a^\dagger + a\right)\left(\sigma^+ + \sigma^-\right) = a^\dagger\sigma^+ + a^\dagger\sigma^- + a\sigma^+ + a\sigma^-$ and we see we are nearly finished.

The last step requires the cancellation of $a\sigma^-$ and $a^\dagger\sigma^+$, which requires changing shortly to the interaction picture of the system[2]. In this picture the operators pick up a specific time dependence $\hat{O}(t) = \hat{O}e^{i\omega t}$ so that our operator terms become

$$a^\dagger\sigma^+ e^{it(\omega_r+\omega_{qb})} + a^\dagger\sigma^- e^{it(\omega_r-\omega_{qb})} + a\sigma^+ e^{-it(\omega_r-\omega_{qb})} + a\sigma^- e^{-it(\omega_r+\omega_{qb})} \tag{2.7.5}$$

Now we recognize an interaction occurring at high frequencies $\omega_r + \omega_{qb}$ and at low frequencies $\omega_r - \omega_{qb}$. As is done in the Jaynes-Cummings model we neglect the terms at high frequencies, considering their contributions to the evolution of the system to be too fast for consideration. One might also recognize that these operations $a^\dagger\sigma^+$ and $a\sigma^-$ do not conserve energy and for our simplistic view, we can ignore them as physically unrealizable[3]. This is again a rotating wave approximation.

With this we can rewrite our original Hamiltonian into a Jaynes-Cummings form as

$$H_{\mathrm{CQED}} = \hbar\omega_r\left(a^\dagger a + \frac{1}{2}\right) + \hbar g\left(a^\dagger\sigma^- + a\sigma^+\right) + \frac{E_{\mathrm{J}}}{2}\hat{\sigma}_z \tag{2.7.6}$$

where g is the coupling constant

$$g = E_C\frac{C_G}{2e}\sqrt{\frac{\hbar\omega_r}{2C}} = 2e\frac{C_G}{C_\Sigma}\sqrt{\frac{\hbar\omega_r}{2C}} \tag{2.7.7}$$

and we have used equation 2.4.3 to substitute for E_C. The coupling between the resonator and qubit either take energy from the resonator circuit and give it to the qubit, $a\sigma^+$, or take energy from the qubit and give it to the resonator, $a^\dagger\sigma^-$. These interactions will oscillate with time leading to the phenomenon of Vacuum Rabi Oscillations at a frequency $\Omega_{Rabi}^2 = \triangle_{qr}^2 + 4g^2(n+1)$ where n is the Fock state of the resonator, or the number of "photons" in the cavity and $\triangle_{qr}$ is the detuning frequency $\omega_q - \omega_r$.

---

[2]There are three common "pictures" of quantum mechanics, the Schrodinger picture, the Hamiltonian picture, and the Dirac/Interaction picture. In the Schrodinger picture, any time dependence of the Hamiltonian will be accounted for in the state vector $|\psi\rangle$, while in the Hamiltonian picture the dependence is absorbed in the operator $\hat{O}$. In the interaction, or Dirac, picture the time dependence is shared between both the state and the operators.

[3]One should not presume these interactions are impossible, in fact they are possible, but in our simple model we neglect them.

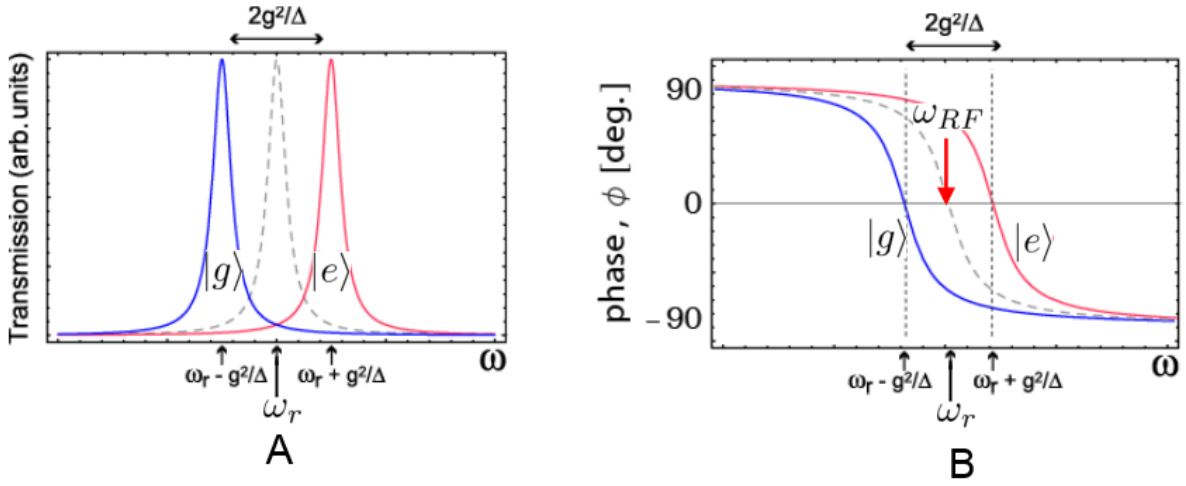

FIGURE 2.8.1. The resonant frequency shift and phase shift, (A) and (B) respectively, of a resonator coupled to a qubit in the dispersive regime

2.8. Measurement of the Qubit-State

As stated in the previous section there are a number of advantages to coupling the qubit to a resonator. One of the reasons is to perform QND type measurements so our goal now is to determine how we can measure the state of the qubit in this system.

As a path to figure out the best way to measure the state of a qubit in this coupled system we first look at how to control the qubit when it is coupled to a resonator. In principle we could create a separate control circuit which interacts with the qubit directly. However, a more efficient system might detune the resonant frequency of the resonator and the qubit, so that when we send a sinusoidal voltage through the resonator to the qubit, the resonator is hardly perturbed and merely degrades the amplitude of the signal before it reaches the qubit. However, this detuning means the coupling between the resonator and the qubit is much weaker and our previously derived Hamiltonian can be simplified further. In the limit that $\triangle_{qr} \gg g$ we can treat the coupling as a perturbation, by transforming 2.7.6 with the unitary transformation $U = \exp\left(\frac{g}{\triangle}\left(a\sigma^{+} - a^{\dagger}\sigma^{-}\right)\right)$ and expanding to second order in g we find the dispersive Hamiltonian to be

$$H_{\triangle_{qr}} = \hbar\left(\omega_r + \frac{g^2}{\triangle_{qd}}\hat{\sigma}_z\right)a^{\dagger}a + \frac{\hbar}{2}\left(\omega_q + \frac{g^2}{\triangle_{qd}}\right)\hat{\sigma}_z \tag{2.8.1}$$

The first term in the Hamiltonian looks like a harmonic oscillator with a frequency shifted by a value of $\pm\frac{g^2}{\triangle_{qd}}$ such that $\omega_r' = \omega_r + \frac{g^2}{\triangle_{qd}}\hat{\sigma}_z$. This is called the ac-stark shift of the resonator cavity. Recalling that $\hat{\sigma}_z$ is correlated to the state of the qubit from 2.7.6, we see that the effective resonant frequency of the resonator, ω_r', when it is coupled to a qubit, is dependent on the state of the qubit. Since we are in the dispersive regime, i.e. the resonant frequency of the resonator and qubit are far detuned, we are free to measure ω_r' to determine the state of the qubit without perturbing the qubit!

Conversely we could rewrite this Hamiltonian as

$$H_{\triangle_{qr}} = \hbar\omega_r n + \frac{\hbar}{2}\left(\omega_q + \frac{g^2}{\triangle_{qd}}\left(2n+1\right)\right)\hat{\sigma}_z$$

were now we see the resonant frequency of the qubit, is dependent on the energy level of the resonator. Thus, if we wanted to measure the energy level of the resonator we could measure the effective resonant frequency of the qubit. This is actually essential if we wish to initially calibrate the values of the Hamiltonian in a newly created circuit.

Thus, to measure the state of the qubit all we have to do is perform some basic spectroscopy on the resonator and we are done. If we were to have computed all of this in the phase basis we would also find a similar phase shift state dependency. These are graphically show in Figure 2.8.1.

2.9. Larger Complexity and Conclusion

At this point we have covered the basics of superconducting quantum circuits. We started with our classical understanding of a resonating circuit and gradually increased the complexity to a fully functional qubit. We have not gone into the full details of this field, for example, neglecting dissipation and decoherence, but attempted only to give a brief overview of the material as to learn the principles of using quantum circuits. In the lab, these qubits have actually been created with various designs, typically, the role of the resonator is played by a linear wave guide which can be approximated as an infinite series of parallel L,C components. Qubits are capacitively coupled to this waveguide and interact via exchange of "photons" with the resonating cavity. This can be seen in Figure 2.9.1.

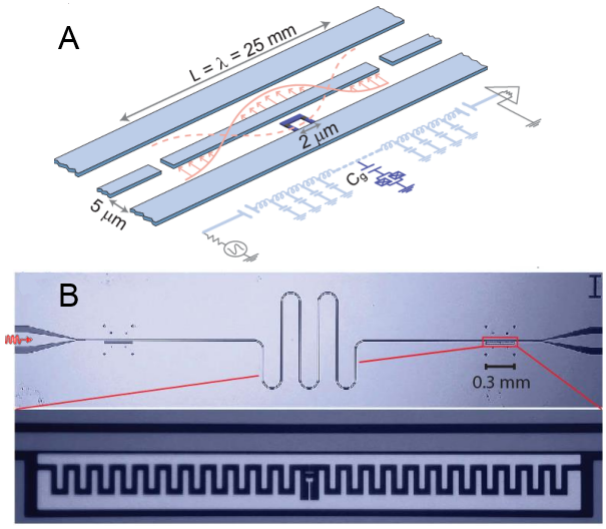

FIGURE 2.9.1. A) 1D transmission line resonator with coupled qubit, B) Actual resonator with coupled qubit, the long squiggly line acts as the resonator cavity and the zoomed in inset, right in the vary middle is the actual Transmon qubit.

At this point in the field, qubit-qubit interactions have been demonstrated with these transmission line qubits as well as a universal set of quantum gates. In fact, all of the DiVincenzo Criteria have been fulfilled most with a high degree. However, a lot of work and advances are required in the field if a real practical quantum system is to be realized. Such things as increasing coherence times of the qubits, increasing the fidelity of gates, decreasing gate operation time, scaling the circuits down while scaling the number of qubits up, possible advances in higher temperature superconductors would be useful as well.

CHAPTER 3

Trapped Ions

One of the most prominent candidates for a physical system realizing quantum information processing is the trapped ion system. In this field, charged atoms, ions, are used to create a qubit and lasers are used to control the state. As we shall see all of the core DiVincenzo criteria have been met with high fidelity and a relatively large number of qubits have been , putting trapped ions arguably at the front of the race for quantum computation.

The first step, of course, will be trapping the ions in a controlled manner for a long period of time in order to use them. This is not the easiest feat because the electrostatic potential for trapping the ions must satisfy the Laplace equation

$$\nabla^2 V = 0 \rightarrow \frac{d^2V}{dx^2} + \frac{d^2V}{dy^2} + \frac{d^2V}{dz^2} = 0$$

There are a number of solutions to this equation, but the general form will normally only allow 2 directions to remain trapped while the third is free. The electrostatic potential would look something like a horse saddle so that the ion in this field would be harmonically trapped in the x, and y, direction but free to fall out of the trap in the z direction. This problem was solved by Wolfgang Paul for which he later received the Nobel Prize. His Paul trap is basically the same saddle potential, but rotated quickly about the axis which passes vertically through the origin. Luckily, since the ions are relatively massive, their acceleration is slow enough that radio frequency rotations of the field is enough to keep the ion at small perturbations around the saddle point. Based off this work the quadrupole ion trap is the standard for this field.

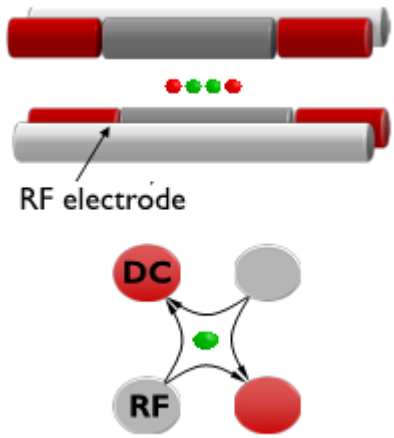

FIGURE 3.0.1. A common Ion Trap

The traditional trap has four long metal rods placed parallel to each other to form a rectangular prism. A static DC field is applied across two opposite corners of the rod while an alternating radio frequency field is applied to the other two. This traps the ions in a string along the central axis through the prism and creates a nearly ideal harmonic potential for trapping.

Once an ion is trapped, then two energy levels of the atomic state need to be used to define the qubit. Since we are working with atoms, the energy level diagrams are rather complex and also depend on the presence of external fields and which atom you use. Two common ions are Calcium and Beryllium both with one valence electron stripped off leaving only a single valence electron in an S orbital configuration. There are either hyperfine qubits which split this ground state into spin states or optical qubits which use two distinct energy levels. The guiding light, however, for choosing the two states is the relaxation time and coherence properties of the two states. Fermi's golden rule and a dipole approximation allow one to calculate the decay time of states as

$$\tau \propto \frac{1}{\omega^3 \left|\langle 0| E \cdot d |1\rangle\right|^2}$$

After two levels have been identified the next requirement is to initialize the qubit. This is done with a technique called **optical pumping** in which a laser is shinned onto the atom of choice and set to a frequency resonant with the $|1\rangle$ state of the qubit and a third excited state in the atom $|e\rangle$. This third excited state is chosen such that it will naturally decay into the $|0\rangle$ state and the transition frequency between $|0\rangle$ and $|e\rangle$ is

different enough from $|1\rangle$ and $|0\rangle$ so that the laser will not excite an electron in the $|0\rangle$ state. After enough waiting time, ~20ns, the electron has a roughly 99.99% chance of being in the ground state.

In a similar manner, measurement of the qubit states can be performed by shinning a laser on the atom with a frequency resonant with the $|1\rangle$ state and another excited state $|e'\rangle$. This excited state is chosen such that the decay of an electron in this excited state goes back to the $|1\rangle$ state and that the transition frequency is not resonant with the $|0\rangle$ state or any other excited state. When the electron decays back into the $|1\rangle$ state it will emit a photon which can be collected. By driving such a transition for a period of time and collecting the number of photons emitted in that time, the ground and excited state of the atom can be identified. Specifically, if a large number of photons are collected then the qubit was in the excited state, but if only a few or no photons were collected then the qubit was in the ground state. This is called the electron shelving method.

The collection of these emission photons is probably the trickiest and least efficient processes in the trapped ion system. The CCD camera or photomultiplier tube used to capture these photons typically only captures a tiny percentage of the total emitted photons. The atom will emit the photon in a random direction and the imaging system will only collect a specific and small solid angle of the total possible angles of emission. This leads to readout times of 100s of microseconds with 1000s of scattering events. However, even with this limitation the measurement process still has a very large fidelity as the relaxation time of the excited states can often be as large as seconds or even minutes.

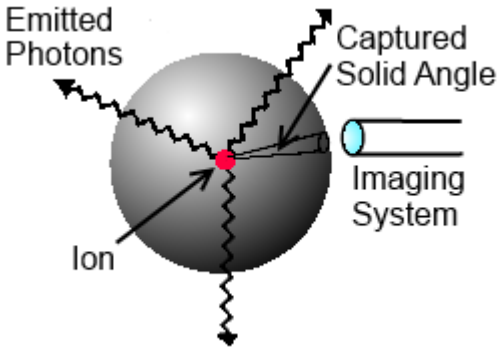

FIGURE 3.0.2. The captured solid angle of emitted photons is small

Now we need coherent qubit control. Trapped Ion qubit control is actually completely equivalent to the Superconducting Circuit case when we coupled the qubit to a harmonic drive. This gave the effective Hamiltonian of 2.6.8. The frequency and phase of the laser cause Rabi oscillations and effectively rotate the qubit around the Bloch Sphere in a very controllable and precise way allowing for arbitrary qubit control.

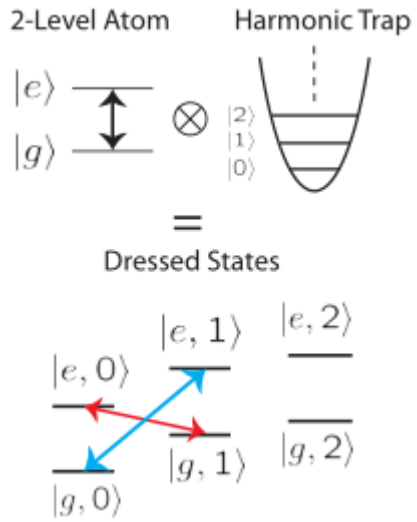

FIGURE 3.0.3. Dressed states of ion in a harmonic trap.

The last and probably most difficult process for trapped ions is the qubit-qubit interaction to create a two qubit controlled gate. There are two main methods to do this, however, both implementations revolve around the use of the states of motion of the ions in the trap to provide the coupling of the qubits. Specifically, the fact that the ions are trapped in a one-dimensional string lattice means that natural vibrational modes will occur. The internal state of the atoms will couple to the phonons in the lattice creating a set of dressed states, much like the cavity QED case. The trap is taken to be harmonic so it acts like a series of springs connecting the ions. In the first implementation by Cirac and Zoller (1995) when the laser is detuned from the atom at a frequency equal to the natural vibrational frequency of the trap, the internal state of the atom becomes coupled with the vibrational state of the string. This causes a frequency shift of the Rabi oscillations of the ions dependent on the number of phonons, ie the vibrational mode, in the trap. In their implementation they create a CNOT gate by first mapping the state of the control bit onto the vibrational state of the lattice. Then a single qubit rotation occurs on the target qubit dependent on the vibrational state of the lattice. Finally, they map the vibrational state of the lattice back onto the original control qubit.

The second implementation was done by Leibfried et al. (2003) in which they used the interaction of the lattice with a standing wave to create an effective CPHASE

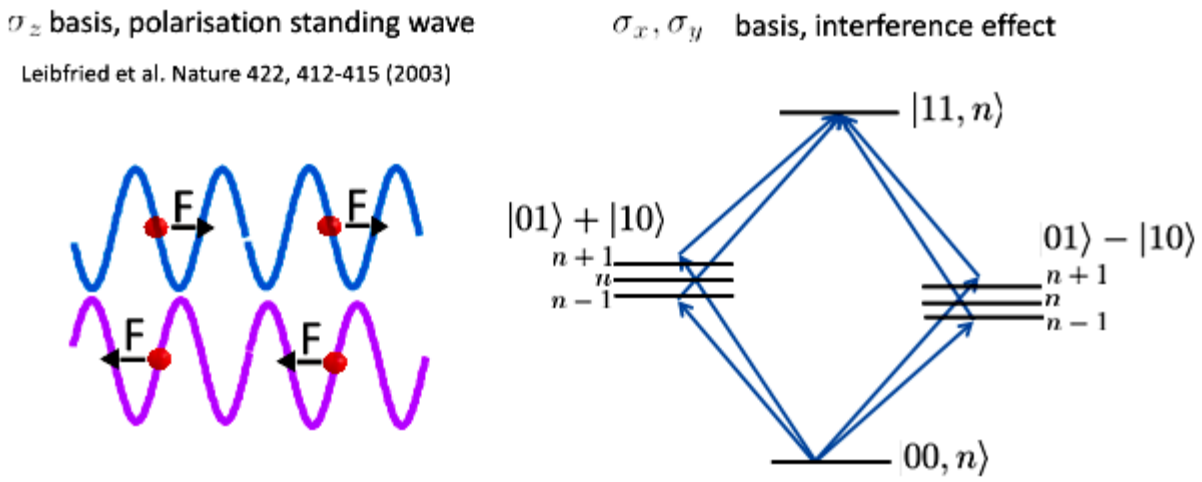

FIGURE 3.0.4. Leibfried CPHASE gate

operation. Specifically, they shine two interfering lasers on the entire lattice of ions. These interfering lasers create a standing wave which applies a force on the ions. Based on the frequency difference of the two lasers there are two possible forces the ions feel. If both ions are in the same electronic state they both feel an identical force. The period of interference is inversely proportional to the the detuning frequency of the lasers and after one period the string returns to its original state. However, if the two ions are in different states then they will feel opposing forces and the stretching mode of the lattice is excited so that the two ions move in opposite directions. After a period of interference this stretching mode will cause the wave function to pick up a phase. The intensity of the light determines how much of a phase is obtained and it is chosen in a way that causes a phase of $\pi/2$ if the ions which are in different states and no phase if they are in the same state. Effectively this interaction creates the gate with matrix

$$G = \begin{bmatrix} 1 & 0 & 0 & 0 \\ 0 & i & 0 & 0 \\ 0 & 0 & i & 0 \\ 0 & 0 & 0 & 1 \end{bmatrix}$$

.

We have now seen the core of the Divencenzo Criteria fulfilled and the other two criteria will be better explained in the student presentations about quantum networking and simulations using trapped ions. The last thing we will discuss here are the next future for Trapped Ions.

The next steps for trapped ions is creating a scalable architecture. Packing more and more qubits into a single string makes the dynamics as well as individual qubit addressing much more difficult. There are already ideas being tinkered with to solve this problem by breaking the string up. Specifically, the ions can be ported around a 2D grid using electrostatic gates. With these gates ions can be physically moved around and brought together to interact when necessary. Also, by distributing entanglement between sections of strings, it is possible to simulate one long effective string of ions. Of course however, this creates new problems that will have to be resolved from both a physics and an engineering perspective. Other advances include moving from a large 4 rod ion trap to an integrated circuit chip design. It is indeed possible to trap ions using a 2D structure, but of course this introduces new difficulties. Also, integrating the lasers and optical capture devices onto a chip is not a simple engineering challenge. Nevertheless, trapped ions have proved to be one of the top contenders for a physical system which can implement quantum information processing. It has demonstrated with large fidelities the DiVencenzo criteria, as well as demonstrated other QIS challenges such as teleportation, super dense coding, error correction, various algorithms and control of the largest number of qubits simultaneously. There is an entire course on trapped ion physics taught at ETH and if you want to get in the field of trapped ion quantum computing, that is probably a great course to take.

CHAPTER 4

Quantum Dots

4.1. What is a Quantum Dot?

Next we look at the field of quantum dots as another possibility for quantum information processing. A quantum dot is a confining potential created within a semiconductor or metal which is capable of trapping a single electron. The potential itself has well defined quantized energy levels which the electron can occupy. The potential can also trap more than one electron and in this way a quantum dot, acts much like an artificial atom. Not too long ago, a physicist would have been very skeptical if you told them you could trap a single electron and coherently manipulate and read-out its spin state, yet today this is quite a common feat.

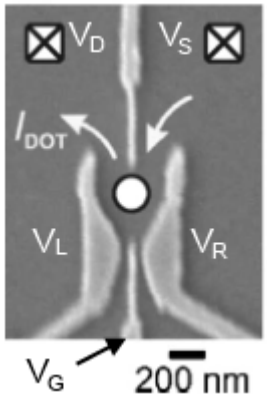

FIGURE 4.1.1. Top view of a single quantum dot

Before we delve into the aspects of manipulating spin's of electrons in quantum dots, we shall first look at the construction of a quantum dot. The basic idea is much like for quantum circuit design and the cooper pair box. We wish to create an island where electrons are confined and which we can control the occupation of the island via a gate voltage. There are a plethora of designs and materials to create a quantum dot, however our discussion here will focus mainly on lateral quantum dots constructed from Gallium Arsenide (GaAs) and Aluminum Gallium Arsenide (AlGaAs) heterostructures, as they are the most common. A layer of silicon doped AlGaAs is placed on top of GaAs. The silicon doping introduces free electrons into the system which tend to accumulate at the interface between the AlGaAs and the GaAs. These electrons are heavily confined to this interface creating a two dimensional electron gas (2DEG) with high mobilities in the plane. On top of this structure are placed some metallic gates which will create electrostatic potentials felt by the 2DEG. These gates deplete the electrons in a particular region creating the quantum dot.

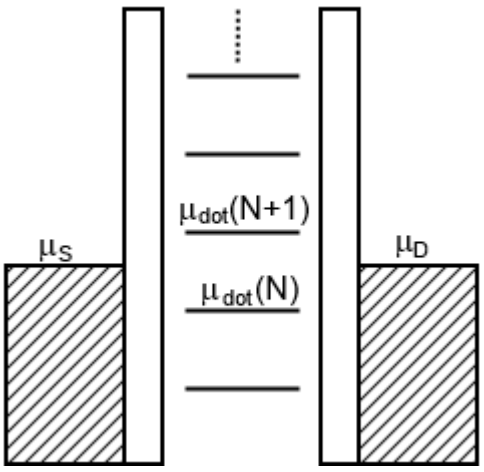

FIGURE 4.1.2. Chemical potential model of a single quantum dot

Figure 4.1.1 shows an electron tunneling microscope picture of a single quantum dot. The light gray parts are the metallic gates, the white circle in the middle shows the location of the quantum dot. The actual 2DEG is typically a few tens of nanometers below this surface. The white boxes in the corners of the picture show the Ohmic contacts which burrow into the structure to make contact with the 2DEG. I_{Dot} shows the flow of electron current from the right side, source, to the left side, drain. V_{R} and V_{L} control the tunneling barrier between the quantum well and the source and drain respectively. V_{G} controls the "depth" of the well.

The relevant physics of the system can viewed very simply. First off we can picture this confining potential much like a particle in a box. The energy levels will be quantized proportional to the square of the energy level, n, and inversely proportional to the mass of the electron and the square of the dimensional length of the box. In addition a Coulomb energy will have to be overcome if we wish to place more than one electron in the well, due to the electrons mutual repulsion. Finally, we can not forget the Pauli-exclusion principle allowing only one electron

per spin state. The exact details of this system are not particularly relevant for our purposes here since we will be working in a cold regime (T<0.5K) such that only the ground state of the well is relevant in the dynamics of the system.

In order to add the effects of the gate voltages we use a simplistic chemical potential model. In this model, depicted in Figure 4.1.2, the chemical potential of the source, drain, and well, depend linearly on the voltage applied to each area. By increasing the voltage across the source and drain we can linearly raise and lower the chemical potential of these parts in the graph. If we change the voltage on the gate then we raise and lower the ladder of states in the quantum dot. The white bars represent the tunnel barriers and the thickness of these barriers is related to the voltage on the left and right gate in Figure 4.1.1. From all of this we get unprecedented control of the system.

4.2. Controlling the Number of Electrons on a Quantum Dot

Now that we know how to create a quantum dot, let us look more specifically at controlling the the population of electrons in our dot. By applying a small source-drain voltage we create a tiny window through which, if an electron state is present in the dot, an electron may move from the source to the drain creating a measurable current. By changing the gate voltage to more and and more negative values, we push the ladder of states in the dot higher and higher. This leads to three different possible scenarios in the chemical potential picture depicted in Figure 4.2.1. In scenario (a) an energy state of the dot falls between the chemical potential of the source and drain so that an electron can tunnel from the source into the dot, then out of the dot into the drain. In this configuration we expect to see a current through the dot. In scenario (b) our ladder of states in the dot is offset from the source-drain window such that tunneling can not occur from the source into the dot. This configuration is known as a coulomb blockade and we would expect to see no net current through the dot, however there are still electrons present in the dot itself. Finally, if we push the gate voltage high enough, we get scenario (c) in which we get a complete depletion of electrons from the dot. Of course there is no net current in this configuration as well. Therefore, if we were to plot the current through the dot as a function of gate voltage, we expect to see spikes of current through the dot when we have reached a special gate voltage corresponding to the (a) configuration. These spikes will be separated by areas of zero current flow when the configuration is Coulomb blockaded. Finally, we should find a point where spikes no longer seem to appear and this suggests to us we have reached the (c) regime. This means the last bump we saw should be the last electron in the dot.

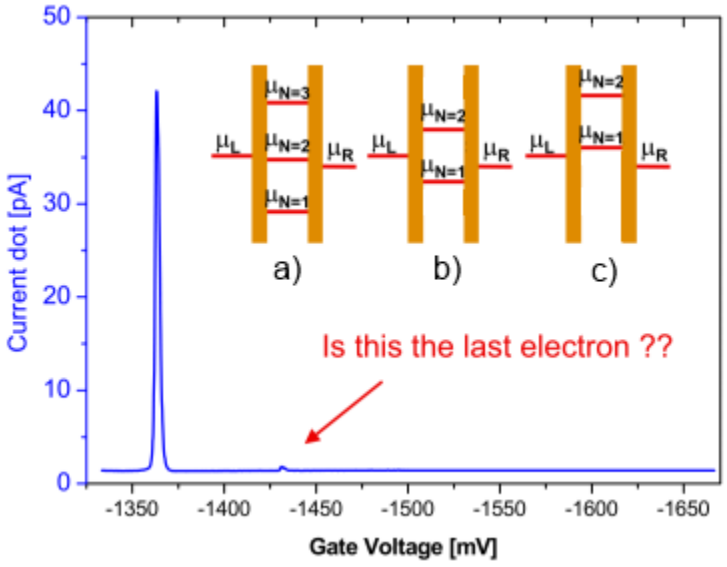

FIGURE 4.2.1. Quantum dot current as a function of the gate voltage

However, we might be a little skeptical that our instruments are sensitive enough to read a single electron tunneling through the ground state of the dot. To verify if we have indeed found this last electron a Quantum

Point Contact is utilized as an extremely sensitive charge sensor. The concept of a Quantum Point Contact (QPC) is actually rather simple. Two regions with high conductance are separated by a "narrow" channel. The "width" of this channel restricts the number of electrons which may pass at that time, thus affecting the net current which may flow between the two regions when a voltage is applied. The QPC is placed spatially close to the dot, such that the effective "width" of the QPC channel is correlated to the presence of electrons in the dot as well as the gate voltage applied on the dot. As the gate voltage is negatively increased, the "width" of the QPC gets proportionally smaller. As the number of electrons increases in the dot, the "width" of the QPC is also increased. Since the presence of electrons in the dot reduces with increasingly negative gate voltages, we expect to see a current through the QPC that decreases as the gate voltage becomes more negative, with small positive bumps. The bumps correspond to an electron suddenly tunneling off of the dot, due to the increased gate voltage and so its constriction on the QPC channel is now gone, effectively increasing the "width". This technique proves to be more sensitive for detecting the presence of charges in the dot and the results of such an experiment are shown in Figure 4.2.2. Now we are confident in determining the number of electrons in the dot.

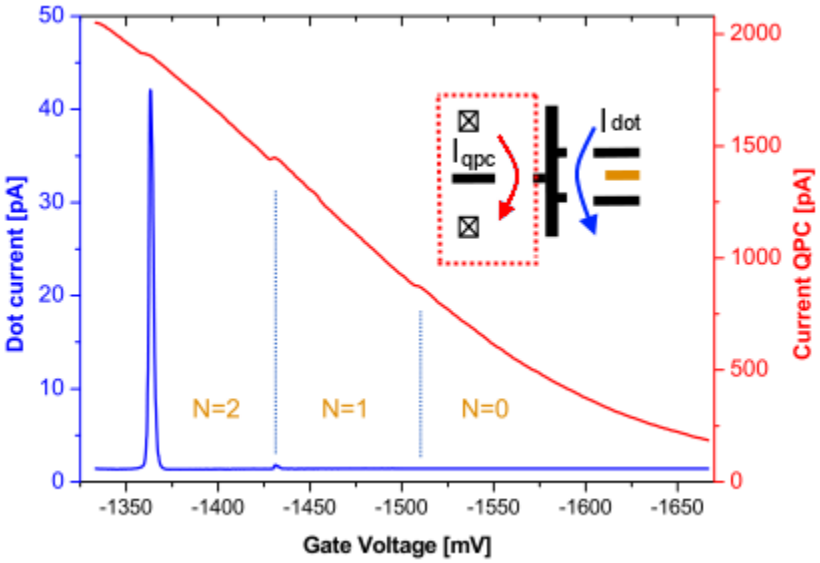

FIGURE 4.2.2. Quantum dot current and Quantum Point Contact current as a function of gate voltage

4.3. Single Electron Spin Qubits

Now that we have complete electrostatic control of our dot, its quite simple to envision a single electron spin qubit. First cool the dot down to low temperatures, split the ground state using an external magnetic field, separating it into a spin up and down state. These two states have much less energy then the charging energy so that only one electron can occupy the dot at any time. Then adjust the voltages on the gate to allow one electron in, only in the lowest spin state, then apply other external magnetic fields to rotate the spin as you please. The spin vector will be your Bloch vector and thus your qubit is complete.

The question now is, how to read the spin state of the electron? There are many ways which have been devised to measure the electron spin state. We will only focus on one of them as it is one of the simplest schemes to understand. One measurement tool we have already present in our dot structure is the quantum point contact which can determine the presence of an electron in the dot, but it does not show anything about the spin of the electron. Some cleaver thought, however, will allow us to create a read-out scheme using the QPC and allow us to determine the spin of the electron. Specifically, if we adjust the levels of the dot during the "read-out" phase such that the higher energy spin state is above the chemical potential of the source, while the lower energy state is below it, then a tunnel event will be correlated with the spin state of the electron. If the electron is in the excited spin state, we would expect to see the electron tunnel off the

dot for a short time, and then see an electron tunnel back in, into the available lower spin energy state. If the electron was already in the ground spin state, then we do not expect to see any tunnel events. Indeed this procedure is done and can visually be seen in Figure 4.3.1.

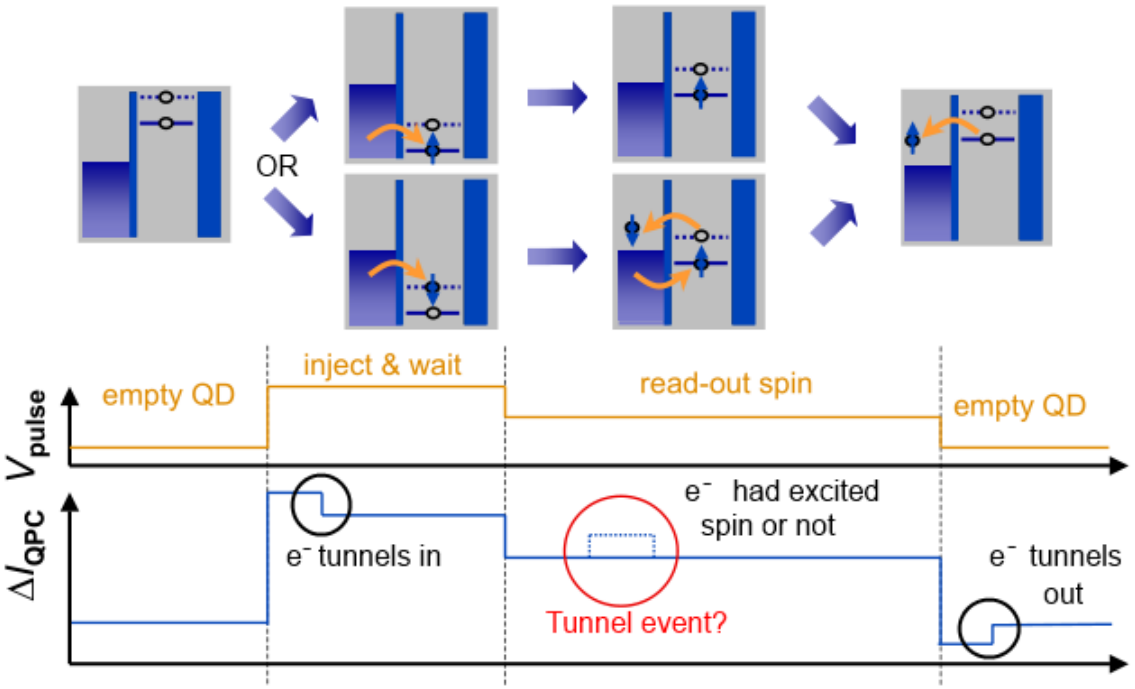

FIGURE 4.3.1. Spin read-out procedure

In the figure we see both the digital read-out as well as the chemical potential picture of each step. Initially the QD is emptied, then a rapid positive increase in the gate voltage drops the dot ladder so both spin states are available. After a short time an electron will tunnel into either the excited or ground spin state of the dot. This can be seen by a quick decrease in the QPC current/conductance. Then the gate voltage is changed again so that the excited spin state is above the chemical potential of the source and we wait to see if a tunnel even occurs. Once enough time has passed, we will either see a tunnel event or not, at which point we know the spin state of the electron. This is called a spin-to-charge conversion readout. Note in these pictures the right tunnel barrier is thick so that the electron does not actually go to the drain. This is for this scheme irrelevant since we do not care about a net dot current, only the QPC current.

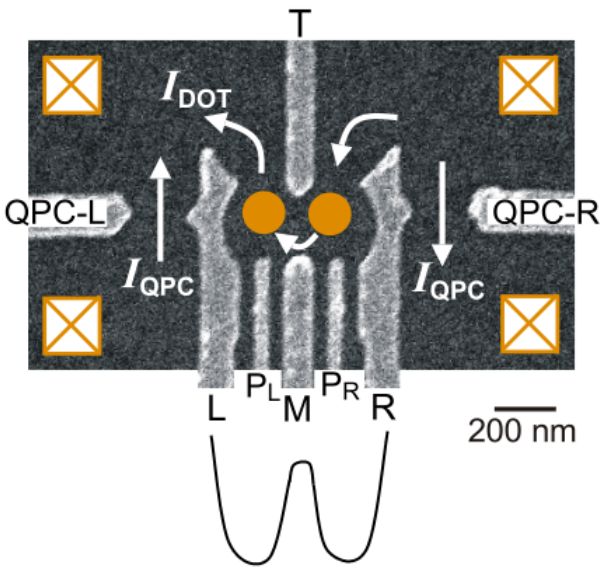

FIGURE 4.3.2. A double quantum dot

The next step is to have qubit-qubit interactions to try and create logic gates. If we place two single electron quantum dots next to each other, we create a double quantum dot, and a natural spin-spin coupling will occur between electrons trapped in the wells. As seen in Figure 4.3.2 the gate structure becomes a little more complex, but is essentially nothing more than 2 single quantum dots placed next to each other with a central tunnel gate, T. The curve underneath

the picture is there to help visualize the role of each gate in the underlying potential. R and L create the tunnel barriers between each dot and the source/drain, while T creates a potential barrier between the two dots. P_L and P_R known as the plungers effectively determine the depth of the left and right well. With all of these electrostatic gates, electrons can be shuffled in, out and between the two dots. Also, with the central tunnel barrier, the interaction between the two dots can be effectively turned on and off.

In this configuration the electrons in each well will form overall singlet, or triplet states in the well. The singlet state has lower energy with a wave function $|S\rangle = 1/\sqrt{2}\,(|\uparrow\downarrow\rangle - |\downarrow\uparrow\rangle)$ while the three degenerate triplet states T_+, T_-, T_0 have wave functions $|T_+\rangle = |\uparrow\uparrow\rangle$, $|T_-\rangle = |\downarrow\downarrow\rangle$, $|T_0\rangle = 1/\sqrt{2}\,(|\uparrow\downarrow\rangle + |\downarrow\uparrow\rangle)$. A simple model for the interaction Hamiltonian is

$$H_{QDint} \approx J_{LR}\sigma_L \bullet \sigma_R \tag{4.3.1}$$

where $\sigma_{L,R}$ is the spin of the electron in the left and right dot, while J_{LR} is the coupling term between the two dots. This coupling term is dependent on the strength of the tunnel barrier between the two dots as well as the "de-tuning factor" which is simply the difference in voltage applied to the left and right plungers.

Greater detail of this system and interaction will be explained in one of the student presentations, since these double quantum dots are actually now used to define a new type of quantum dot qubit which utilize the S and T_0 states to define the ground and excited state of a single qubit. The reasons for doing this should also be explained in the presentation, however its sufficient to know that these singlet-triplet qubits are less susceptible to electrostatic noise in the circuit. As for the single electron spin qubit, when the interaction is turned on an effective SWAP gate is realized where the spin of the each electron flips, effectively "swapping" the two electron spin states.

These qubits have long relaxation times on the order of milliseconds, and dephasing times as high as microseconds, while the interaction times are faster than nanoseconds. This is ideal for quantum computational applications. However, quantum dots and their application to quantum computation are still relatively new compared to quantum circuits, trapped ions and even older still, nuclear magnetic resonance and photon based designs.

CHAPTER 5

Linear Optics Quantum Computing

Many of the first experiments in quantum computation were done with photons, including quantum teleportation. The reasons for this are because photons, in many ways, are the most readily available qubit found in nature. Vertical and horizontal polarization form a natural orthogonal basis for the qubit state. They only weakly interact with the environment and therefore have extremely long coherence times while at the same time they travel extremely quickly with little attenuation. This makes them ideal flying qubits.

On top of the natural characteristics of photons which makes them ideal qubits. The fact that optics has been a formal field for quite some time in physics, well before the notion of quantum information processing, means that there was already a wealth of knowledge and tools readily available for the experimenters. The use of dielectric materials and polarizes allow for the control of the phase and polarization of photons. The use of beam splitters, lenses, mirrors and resonator cavities allow control of the physical path of photons. Also, relatively efficient photon detection methods were ready and waiting for use in quantum computing systems.

Unfortunately, there are a few crucial drawbacks to photon based systems and that is the nearly non-existent photon-photon interaction and the difficulty for deterministic entanglement and creation of single photon sources for the necessary Ancilla bits. This makes 2 qubit gates difficult to realize and drastically reduces the process fidelity of many quantum protocols. Though this drawback does not make it impossible to create such gates or accomplish such protocols, it does however change the paradigm of linear optic quantum computing to an inherently non-deterministic form of computing. Nevertheless, proper error-correction, physical engineering and the rapid speed at which optical circuits can operate all keep linear optic quantum computing within the realm of possibility for future quantum computing success.

To begin, as always, we start by defining the qubit in a photon based system. There are a number of possibilities for defining a qubit with a photon. The three major types are the single-rail, dual-rail and polarization qubits. The single-rail architecture is conceptually quite easy, the presence or absence of a photon in a spacial location defines the logical $|1\rangle$ and $|0\rangle$ states respectively. This architecture allows for deterministic creation of entangled states, but it has the drawback of only allowing for probabilistic single qubit manipulations. For this reason, this type of qubit is not used very often. In the dual-rail system the photon's path at a beam splitter is used to define the qubit, while in polarization qubits the internal polarization of the photon is used. These two types of qubits are actually mathematically equivalent as we will see in a moment.

First, we will consider a photon incident on a beam splitter. Formally, the left and bottom paths are defined as the two input ports, while the top and right paths are the two output ports as seen in Figure . If the beam splitter is assumed to be lossless then the reflection coefficient of the beam splitter is $R = \sin^2\theta$ and the transmission coefficient is $T = 1 - R = \cos^2\theta$ then the ports input and output relations are given by

$$\begin{aligned} a^\dagger_{out} &= a^\dagger_{in}\cos\theta + ie^{-i\phi}b^\dagger_{in}\sin\theta \\ b^\dagger_{out} &= ie^{i\phi}a^\dagger_{in}\sin\theta + b^\dagger_{in}\cos\theta \end{aligned} \tag{5.0.2}$$

where ϕ is a controllable relative phase shift induced during reflection. The angles θ and ϕ are the equivalent angles of rotation on the Bloch sphere and a_{out} and b_{out} are the computational $|0\rangle$and $|1\rangle$ states respectively.

This convention uses creation and annihilation operators on the spacial (ports) of a and b, hence the daggers denoting the creation of an a port photon. Specifically, if $\emptyset$ denotes the vacuum state and $|\emptyset\emptyset\rangle$ represents the vacuum state of either the two input ports or two output ports then

$$a^\dagger|\emptyset\emptyset\rangle = |\emptyset 1\rangle \qquad\qquad b^\dagger|\emptyset\emptyset\rangle = |1\emptyset\rangle$$

As an example we have the 50/50 beam splitter, where $R = 0.5 \rightarrow \theta = \frac{\pi}{4}$ and we use $\phi = \frac{\pi}{2}$. This beam splitter would then transform $a^\dagger \rightarrow \frac{1}{\sqrt{2}}\left(a^\dagger + b^\dagger\right)$ and $b^\dagger \rightarrow \frac{1}{\sqrt{2}}\left(-a^\dagger + b^\dagger\right)$ so that $U_{BS} = \frac{1}{\sqrt{2}}\begin{bmatrix} 1 & 1 \\ -1 & 1 \end{bmatrix}$.

Another important element is the single port phase shifter. Any transparent material with a different index of refraction compared to the usual medium of transport will cause a phase shift of the incident photon. A phase shifter acts only on one particular port so that if we placed a phase shifter in the b_{out} port then the phase shifter would do something like

$$\begin{pmatrix} a^\dagger \\ b^\dagger \end{pmatrix} \rightarrow \begin{pmatrix} 1 & 0 \\ 0 & e^{i\Phi} \end{pmatrix} \begin{pmatrix} a^\dagger \\ b^\dagger \end{pmatrix}$$

As stated previously there are also qubits which utilize the internal polarization to define the qubit. If we use vertical and horizontal polarization as our logical $|0\rangle$and $|1\rangle$ then by using wave plates we can have arbitrary rotation of the polarization vector. A wave plate is a birefringent material which means it has a refractive index dependent on the polarization and direction of incident light. The material has an internal fast and slow axis each with a respective index of refraction $n_{Slow} > n_{Fast}$. This induces a phase shift between components parallel to the slow and fast axis such that

$$\phi_{S,F} = k_{S,F}d = \frac{v_{S,F}}{c}d = \frac{k}{n_{S,F}}d$$

If the polarization vector of an incident ray makes an angle θ with the fast axis of the wave plate and the phase angle $\phi = \phi_F - \phi_S$ is induced during a propagation distance d through the wave plate, then the general wave plate relations are

$$\begin{aligned} a^\dagger_{H,out} &= a^\dagger_{H,in}\cos\theta + ie^{-i\phi}a^\dagger_{V,in}\sin\theta \\ a^\dagger_{V,out} &= ie^{i\phi}a^\dagger_{H,in}\sin\theta + a^\dagger_{V,in}\cos\theta \end{aligned} \tag{5.0.3}$$

where the H and V subscripts denote the horizontal and vertical components respectively. With these waves plates arbitrary single qubit manipulation are also possible.

By comparing equations 5.0.3 and 5.0.2 it should be obvious that polarization and dual rail qubits are mathematically equivalent. These two types of qubits can be interchanged through the use of a Polarizing Beam Splitter, which as the name suggests splits an incident beam into two polarized beams.

Now that we have the different types of qubits and shown that single qubit manipulation is possible, we move to the subject of 2 qubit gates. Unfortunately, photons do not directly interact and this fact is at the heart of the problems with linear optic quantum computing. Implementing a two qubit gate where photon qubits interact with each other is not a natural process. Many strategies have been conceived to try and get around this issue, but they all have varying limitations. The most widely used idea, so far, is the KLM scheme which can implement 2 qubit gates in a probabilistic manner.

The core of the KLM architecture involves the Hong-Ou Mandel effect and the Bosonic nature of photons. Returning to the 50/50 beam splitter we consider what happens when two photons are incident at the same time. Using the beam splitter relations we find that

$$\begin{aligned} U_{BS}a^\dagger b^\dagger |\emptyset\emptyset\rangle &\rightarrow \frac{1}{\sqrt{2}}\left(a^\dagger + b^\dagger\right)\frac{1}{\sqrt{2}}\left(-a^\dagger + b^\dagger\right)|\emptyset\emptyset\rangle \\ &= \frac{1}{2}\left(-a^{\dagger 2} + b^{\dagger 2}\right)|\emptyset\emptyset\rangle \\ &= \frac{1}{\sqrt{2}}\left(|2\emptyset\rangle - |\emptyset 2\rangle\right) \end{aligned}$$

and what we see here is photon bunching. Both photons are guaranteed to exit the same port. This is the Hong-Ou Mandel effect and it is used in conjunction with non-linear sign gates to create 2 qubit gates.

A non-linear sign gate, NS, performs the following transformation on incident photons

$$\alpha|0_N\rangle_{in} + \beta|1_N\rangle_{in} + \gamma|2_N\rangle_{in} \rightarrow \alpha|0_N\rangle_{out} + \beta|1_N\rangle_{out} - \gamma|2_N\rangle_{out}$$

where $|n_N\rangle$ denotes the number of photons in the port. There are a couple of different ways to physically implement a non-linear sign gate, but unfortunately they are all probabilistic. The NS gate proposed in the KLM scheme use 3 beam splitters and 2 detectors as seen in Figure . The transmission coefficients for the first and last splitter are roughly 85% while the middle splitter has a transmission coefficient of 17%. The

NS gate will perform the transformation properly if a single photon is detected in the upper detector and no photon is found in the lower detector. With a general input state the probability of success is 25%.

Now we can implement the CPHASE gate as seen in Figure . First we note that this uses two dual-rail qubits. The top qubit has a state $|ab\rangle$ where a and b define the ports and the computational basis values are defined such that $|0\rangle_{comp} = |1\emptyset\rangle$ while $|1\rangle_{comp} = |\emptyset 1\rangle$. The bottom qubit has the reverse such that the general state $|cd\rangle$ defines computational basis states $|0\rangle_{comp} = |\emptyset 1\rangle$ and $|1\rangle_{comp} = |1\emptyset\rangle$.

Now if we look at the gate as a whole, we have a beam splitter, NS gate followed by another beam splitter acting on the middle photons. If our input in the computational basis is $|00\rangle_{comp}$ then it should be clear the gate does nothing, since there are no photons in the middle and the photons on the outside just pass through. For the input states $|01\rangle_{comp}$ and $|10\rangle_{comp}$, 2 photons will never arrive at the NS gate so it does nothing special. There is a 50% chance these states remain exactly as they were and a 50% chance to become non-logical qubit states such that one of the qubits is in the general mode state $|\emptyset\emptyset\rangle$ and the other in the state $|11\rangle$. Finally with the computational basis input state $|11\rangle_{comp}$ we get

$$
\begin{aligned}
|11\rangle_{comp} &= |\emptyset 11\emptyset\rangle = |\emptyset\rangle \otimes \left(a^\dagger b^\dagger |\emptyset\emptyset\rangle\right) \otimes |\emptyset\rangle \\
U_{BS} &\rightarrow \frac{1}{\sqrt{2}} \left(|\emptyset\emptyset 2\emptyset\rangle - |\emptyset 2\emptyset\emptyset\rangle\right) \\
NS &\rightarrow -\frac{1}{\sqrt{2}} \left(|\emptyset\emptyset 2\emptyset\rangle - |\emptyset 2\emptyset\emptyset\rangle\right) \\
&= |\emptyset\rangle \otimes \frac{1}{2} \left(b^{\dagger 2} |\emptyset\emptyset\rangle - a^{\dagger 2} |\emptyset\emptyset\rangle\right) \otimes |\emptyset\rangle \\
U_{BS} &\rightarrow |\emptyset\rangle \otimes \frac{1}{2} \left(\frac{1}{2} \left(-a^\dagger + b^\dagger\right)^2 |\emptyset\emptyset\rangle - \frac{1}{2} \left(a^\dagger + b^\dagger\right)^2 |\emptyset\emptyset\rangle\right) \otimes |\emptyset\rangle \\
&= |\emptyset\rangle \otimes \left[\frac{1}{4} \left(\underline{a^{\dagger 2} + b^{\dagger 2}} - 2a^\dagger b^\dagger \underline{-a^{\dagger 2} - b^{\dagger 2}} - 2a^\dagger b^\dagger\right) |\emptyset\emptyset\rangle\right] \otimes |\emptyset\rangle \\
&= -|\emptyset 11\emptyset\rangle = -|11\rangle_{comp}
\end{aligned}
$$

This is our desired CPHASE operation. It can be shown that the probability of success of this gate is equal to the probability of success of the NS gate squared. If we use the NS gate from the previous paragraph then this gate has a probability of $1/16$ for success.

There is one final process which we shall discuss here as it is a common practice for creating entangled ancilla photons. Many quantum protocols and algorithms require initially prepared entangled states, especially maximally entangled bell states. Previously we discussed the teleportation protocol and found that entangled states could be generated using Hadamard gates and a CNOT gate. This is possible with photons based on what we have already discussed, but a second option for creating bell states is using natural parametric down-conversion. In non-linear optical media, that is media which have polarizations that do not respond linearly to externally applied electric fields, an incident photon can sometimes split into two photons. This conversion conserves energy, momentum and polarization of the incident photon. A 351 nm photon may split into two 702 nm photons. The scattering trajectories of the photons create overlapping cones from the incident plane. The conservation of momentum and polarization will make it so that if one of the photons is at the top of one cone with Vertical polarization, the other photon will be at the bottom of the other cone with horizontal polarization. The places where the cones overlap correspond to maximally entangled photons generating the anti-symmetric bell state $|\Psi^-\rangle = \frac{1}{\sqrt{2}} \left(|01\rangle - |10\rangle\right)$. The use of a wave-plate can then convert this into any of the other bell states. This photon pair can then be used as entangled qubits in any quantum protocol requiring ancilla entangled photon qubits. Typically, Beta Barium Borate (BBO) is used as the non-linear medium. Of course the scattering events are all probabilistic making this a non-deterministic process as well.

By this point the non-deterministic nature of linear-optic quantum computing should be apparent. As stated previously this does not completely cripple quantum information processing using photons it merely increases some of the engineering difficulties with this physical system. However, the true power of photon processing is likely to be in its transportation properties. As it stands now, no physical system can transport quantum information like a photon can and its ease of implementation with already available fiber-optic cable makes quantum networking with photons one of the most viable and appealing options. It may be

likely to see a future in which quantum computers are realized on some physical system such as trapped ions, superconducting circuits, or something else, but that the computers are networked via photon based systems. This hybridization requires the conversion of one type of qubit into photon based qubits. The student presentations on trapped ion quantum networking will have more information about this process using photons to entangle physically distant ions.

CHAPTER 6

NMR

Nuclear Magnetic Resonance was the pioneer physical system for quantum computing. Being the pioneer, it developed many of the techniques used in the other physical systems discussed so far. Unfortunately, the limitations of liquid NMR techniques make it a poor candidate for ideal quantum computation as we shall see in a moment. However, recent developments in Nitrogen-Vacant diamond crystals (N-V centers) may revive NMR as a possible candidate for quantum computing.

NMR systems define the qubit by using the Zeeman effect to split the spin states of spin 1/2 nuclei. By placing such a molecule in an external magnetic field the degeneracy of the up and down spin states is lifted and the qubit ground and excited state are defined. The general Hamiltonian is

$$H_{1/2} = -\hbar\gamma B_0 I_z = \begin{bmatrix} -\hbar\omega_0/2 & 0 \\ 0 & \hbar\omega_0/2 \end{bmatrix}$$

where B_0 is the external magnetic field in the z-direction, γ is the gyromagnetic ratio of the nucleus and I_z is the angular momentum operator in the z-direction. This operator is related to the Pauli operators by $\sigma_i = 2I_i$ where $i = x, y, z$. The energy separation between the two spin states is characterized by the Larmor frequency $\omega_0/2\pi$ which is the angular frequency of the rotation of the nuclear magnetic spin vector around the magnetic field axis.

This Hamiltonian and the dynamics of the NMR system are identical to the quantum dot system. However, now that we are using nuclear spin instead of electron spin, the precession frequencies are roughly 1000 times slower due to the much great mass of the nucleus compared to the electron. Also, the gyromagnetic ratio of each species of nucleus are uniquely different and distinguishable. On top of that a molecule with many nuclei of even the same species typically have distinct frequencies as well, known as the chemical shift c_i. In this way a complete NMR molecule such as that shown in Figure 6.0.1 can be described by the Hamiltonian

Nucleus	$\omega_0/2\pi$(MHz)
^{1}H	500
^{2}H	77
^{13}C	126
^{15}N	-51
^{9}F	470
^{31}P	202

TABLE 6.0.1. Larmour frequencies (qubit level seperation) of common NMR nuclei.

$$H_{nuc} = -\sum_{i=1}^{n} \hbar(1 - c_i)\gamma_i B_0 I_z^i = -\sum_{i=1}^{n} \hbar\omega_0^i I_z^i$$

Table 6.0.1 shows typical values of Larmour frequencies for various nuclei, while the graph in Figure 6.0.1 shows the relevant chemical shifts for the Fluorine nuclei of the complex molecule also depicted in the figure. This data is obtained by resonant spectroscopy on the molecules.

For single qubit rotations, an electromagnetic field perpendicular to the z axis is used to drive the spin vector around the Bloch sphere. In a similar method used to derive equation 2.6.8 we find the control Hamiltonian to be

$$H_{control} = -\hbar\left(\omega_0 - \omega_d\right) I_z - \hbar\omega_1 \left[\cos\phi I_x + \sin\phi I_y\right]$$

and we see again that the phase of the driving field will cause rotations of the spin vector about the x and y axes, so that we have complete single qubit control.

Luckily, nuclear spin states naturally interact via two methods, which make qubit-qubit interactions relatively easy to do. The first interaction occurs via a physical proximity and a natural magnetic dipole-dipole interaction. The second method is indirectly through shared electrons in chemical bonds. In the most simplest case, though a case not to difficult to achieve, both of these interactions can be modeled by the

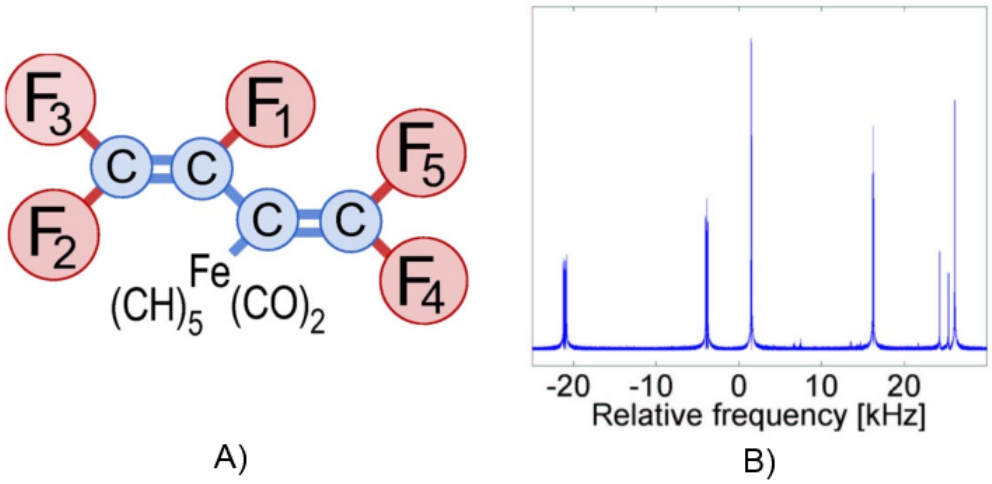

FIGURE 6.0.1. A) A complex molecule used as a 5 qubit processor for NMR B) The relative i.e. zeroed about 470 MHz resonant spectrum of the 5 Fluorine nuclei

Hamiltonian

$$H_J = \hbar \sum_{i<j}^{n} 2\pi J_{ij} I_z^i I_z^j \tag{6.0.4}$$

which basically states that one magnetic spin feels the presence of another by a constant factor, J. Since the interaction is spin state dependent, i.e. if I_z^j is in the 0 or 1 state, this creates energy shifts of one spin state dependent on all of the other spin states. Figure illustrates these relative shifts for 2 interacting spins and the 5 interacting Fluorine spins of the complex molecule in Figure 6.0.1.

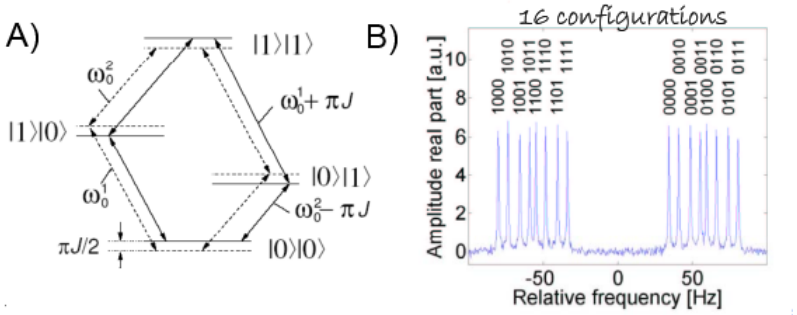

FIGURE 6.0.2. Shifted energy levels due to spin coupling of qubits. A) Shifts due to the presence of 1 other nuclei B) the 16 shifts of 1 F nuclei due to the presence of the 4 other F nuclei of the molecule depicted in Figure 6.0.1

Using this interaction a CNOT gate can be constructed via the following pulse sequence. First, applying a 90^{O} rotation about the y-axis on the target qubit, in order to bring it to the equator. Then it is allowed to naturally precess, and the precession frequency will be shifted based on the spin state of the other molecule via equation 6.0.4. The shift will cause it to rotate faster or slower so that after a time $\frac{J_{ij}}{2}$ the spin vector will either be along the positive or negative y-axis. Then another 90^{O} rotation about the x-axis is applied and this will bring the spin vector back to the z-axis in either the 1 or 0 state dependent on the state of the other qubit.

One obstacle to NMR is the fact that a single molecule represents the quantum processor, but the experiment uses a liquid of roughly $10^{26}$of these molecules to produce a large enough signal for detection.

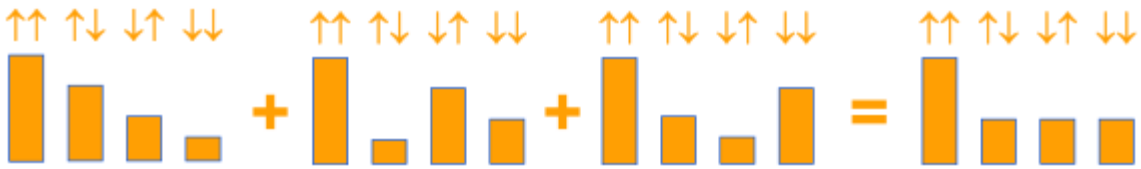

FIGURE 6.0.3. Effective Pure State Preparation for Liquid NMR Quantum Computing

The measured output signal will then be the result of 10^{26} independent quantum computers running an algorithm in parallel and all of these results will show up in the output signal. This liquid (to be a liquid) can rarely be cooled to low enough temperatures to guarantee all the processors are in their ground state. This means that the input of the algorithm will not be a pure state but a mixture of state with a statistical distribution of the various possible energy states of the system. It seems hard to have a deterministic output when the input itself is not deterministic.

To get around this problem and effectively initializing a pure quantum state of N qubits, $\left(2^N - 1\right)$ (later this was improved to $\left(2^N - 1\right)/N$) experiments are performed and the results are averaged. In these experiments, *the non-ground states are cyclically permuted* using standard CNOT and SWAP gates on the qubits. In this way the average output of the experiments will effectively cancel the contributions from the non-ground states and only the result from the desired pure ground state will remain. This is most easily understood using the 2 qubit example in Figure 6.0.3. There are 4 possible energy states for the 2 qubit system with an exponentially decaying occupation number. By swapping the non-ground states and averaging the result, the net effect will be a result from only the desired ground state. This effectively makes the system appear quasi-cold and is called quantum bulk computing.

There are a number of other obstacles to NMR QC, which to various degrees were overcome including overcoming undesired crosstalk between qubits, increasing the coupling between distant qubit nuclei, specific qubit addressing and the inability to "turn off" the coupling between qubits. Many of the techniques used to solve these problems including pulse shaping, echo refocusing, composite pulses etc were later adapted to other architectures. However, the largest draw back to liquid NMR is the issue of scalability.

Scalability of liquid NMR is really the nail in the coffin for this field. The coherence time tends to decrease with larger molecule size. Finding or creating ideal molecules with larger number of usable qubits is difficult. Noise also tends to increase with molecule size and complexity. For any quantum system to truly be scalable each component of the system must have a probability of failure below some maximum value to produce a reliable quantum computing system. This is a consequence of error correction coding and implementation techniques. This threshold error probability is roughly around 10^{-4} and unfortunately, as of yet, has not been achieved in liquid NMR. This threshold has been achieved in most of the other architectures, making them much more promising avenues for quantum computing.

Finally, it has also been argued that many liquid NMR experiments, due to a lack of true entanglement of the qubits in the system, are not truly quantum systems. Entanglement is assumed to be one of the core criteria for a real quantum computer and it suggests that liquid NMR might only be a quantum simulation on a classical computer.

All in all, Liquid NMR has successfully implemented a number of quantum algorithms with a high degree of control. It has certainty left its mark on the field of quantum computation by contributing numerous experimental techniques and though liquid NMR may not be an ideal candidate for a future quantum computing architecture, there is some hope for NMR in the new area of Nitrogen-Vacant crystals or other similar point defect crystals.